PHENOTYPIC ANALYSIS OF *MAGNAPORTHE ORYZAE* MUTANTS: A VIEW INTO COMPONENTS OF mRNA DECAY

by

Ericka Veliz

A thesis submitted to the Faculty of the University of Delaware in partial fulfillment of the requirements for the degree of Master of Science in Plant and Soil Sciences.

Spring 2018

PHENOTYPIC ANALYSIS OF *MAGNAPORTHE ORYZAE* MUTANTS: A VIEW INTO COMPONENTS OF mRNA DECAY

by

Ericka Veliz

Approved: _____
Nicole Donofrio, Ph.D.
Professor in charge of thesis on behalf of the Advisory Committee

Approved: _____
Erik Ervin Ph.D.
Chair of the Department of Plant and Soil Sciences

Approved: _____
Mark W. Rieger, Ph.D.
Dean of the College of Agriculture and Natural Resources

Approved: _____
Ann L. Ardis, Ph.D.
Senior Vice Provost for Graduate and Professional Education

ACKNOWLEDGMENTS

I wish to thank the members of my committee for joining me in this scientific journey. First and foremost, I wish to thank James Sweigard for all his contributions to my research, including the use of his laboratories; Nicole Donofrio, thank you for your guidance throughout my discovery of who I wanted to become as a scientist; and Pamela Green and Janine Sherrier, I thank you for your support and encouragement. Anne Carroll, I sincerely thank you for your knowledge and expertise you shared with me. I'd like to acknowledge Susan Jeffrey for her assistance and expertise throughout this research. To the Donofrio Lab students, thank you for stepping in to help; I thank you for all your efforts. To the DuPont labs and personnel, thank you for your resources, expertise, and guidance throughout this process.

This thesis is dedicated to my son, Colby Smith Jr. Thank you for your patience, encouragement, and for simply spending your childhood in a laboratory with me; your trajectory in science is almost inevitable. This is also dedicated to the memory of Janet Rice, the person that motivated this pursuit to its completion.

TABLE OF CONTENTS

LIST OF TABLES

LIST OF FIGURES

ABSTRACT

Magnaporthe oryzae is a filamentous fungus responsible for causing rice blast disease. Given this disease can cause yield losses of 90% during epidemic seasons, the importance of studying this organism's pathogenicity is critical to farmers as the need for rice has increased for an exponentially growing global population. Whole genome studies in this organism have revealed genes with putative roles in virulence. The specific focus of my research is to examine gene regulation by mRNA degradation as one such virulence control mechanism through the analysis of *XRN1* and *CAF16*, components in mRNA degradation. The exoribonuclease, *XRN1*, moves in a 5' to 3' manner to digest target mRNAs while *CAF16* is a subunit within the CCR4-NOT1 complex that deadenylates the target mRNA. We generated targeted deletion mutants of *XRN1* (*⧋xrn1*) and of *CAF16* (*⧋caf16*) for use in various assays to determine their phenotypic response. Mutants were grown in several stressors (i.e. ROS, nitrogen starved, osmotic stress) as well as non-stressors (i.e. complete media) and analyzed through growth rates. Results show that none of these stressors affect the mutants' ability to grow, indicating that these genes are not critical for growing under stressful conditions. Molecular profiling of the mutants under these stress conditions revealed inconsistent results regarding expression of *XRN1* in *⧋caf16* and vice versa. Expression of two additional genes involved in mRNA degradation pathways, *DCS1* and *POR1*, were measured to determine if there was a decrease in expression in *⧋xrn1*. In the absence of *XRN1*, the data revealed an increase in expression in both genes thereby suggesting both *POR1* and *DCS1* are involved in mRNA degradation, as previous studies in yeast suggested. Finally, mutants were inoculated onto a *M. oryzae* susceptible cultivar of barley to determine phenotypic differences. Data suggests

reduced virulence in ⊿*xrn1* as there were lesser, smaller lesions on the inoculated plant leaves. This phenotypic analysis suggests that *XRN1*, a component in mRNA degradation, is related to virulence, and likely works together with *DCS1* and *POR1* to mediate mRNA degradation. How mRNA degradation and virulence in this pathogen are linked, are fascinating subjects for a future study.

Chapter 1

INTRODUCTION

Magnaporthe oryzae, a filamentous ascomycete, primarily infects cultivars of rice and several other varieties of grasses [1]. With no exact estimate of its yield losses due to other disturbances, such as pests and abiotic factors, infections still cause a critical issue to farmers around the world. Some infections have yielded loses of over 90% in epidemic seasons, and 10-30% in non-epidemic seasons [2]. Rice composes about 23% of the calories consumed by the global human population, and is most critical to the countries in Asia where over half of the world's population resides [1]. With population models projecting 9 billion people by 2050, the demand for rice will need to be increased to 525 million tons, which is about 24% more than currently generated, by 2050 while competing with decreasing availability of land due to housing and industry [3]. The amount of rice lost due to this pathogen has the potential to feed up to 60 million people [4]. Current control measures have only lasted about 2-3 growing seasons before it is met with resistance, thereby increasing costs to ultimately the farmer as they resort to an increased use of fungicides [1]. The need to understand this plant-pathogen interaction is critical to the course of a sustainable solution for the future production of rice.

1.1 *Magnaporthe oryzae* and its Life Cycle

Classified as a hemibiotroph, *Magnaporthe oryzae* infects rice plants and can infect at all stages of development as well as every part of the plant (i.e., leaves, stems,

nodes, panicles and even roots) [1]. Infection primarily occurs as a result of sporulating lesions from an infected plant and from vegetative growth. Vegetative growth typically occurs on dead residue from a previously infected crop, seed, or growth on other grass species such as finger millet, small millets, barley, and wheat [1,5]. Dispersal of conidia occurs by wind or dew-drop splash and leads to contact between the conidia and the aerial surface of a rice or barley plant [6]. This three-celled structure, called conidium (plural: conidia) contains a unique spore tip mucilage that allows adherence to the surface of the leaf [7]. This spore tip is made up of a glycoprotein and secretes this adhesive substance from the top of the conidium following initial contact to the surface of the leaf [8]. The presence of water is critical to the germination of *M. oryzae*. Once germination occurs, a germ tube develops and at this stage, the sensing of various physical and chemical stimuli induces the formation of the appressorium [2]. Appressorial formation requires a hard, hydrophobic surface, often responding to cutin monomers, or the waxy component that makes up the leaf cuticle, on the leaf surface to assist with development. The appressorium has a cell wall that is unique in that it is chitin-rich and contains a layer of melanin, which acts as a barrier as the turgor pressure builds [1]. This turgor reaches pressures of up to 8 megapascals (MPa) while building up a high concentration of solutes, typically glycerol or mannitol, inside the cell in response to hyperosmotic conditions, resulting in a penetration peg directly penetrating through the leaf cuticle [4]. The emergence of the penetration peg breaks through the leaf cuticle and the fungus passes through a biotrophic phase before producing necrosis on the plant resulting in the lesions known as rice blast disease. Taking advantage of the host plant cell's ability to communicate via plasmodesmata, the pathogen moves from

cell to cell gaining nutrients [1]. This type of invasive growth within the plant host occurs at the biotrophic stage and then as lesions are more evident in the host, the fungus becomes necrotrophic, hence its hemibiotrophic classification [1]. Under conditions of high humidity, lesions caused by *M. oryzae* sporulate rapidly spreading the disease at a high rate throughout the plant population. The entire infection cycle takes about 5-7 days, which is why infection spreads rampantly in one growing season [2]. One lesion can produce about 2000-6000 conidia per day for 14 days during one growing season and conidia have the potential to disperse 1 meter or more [9].

Different strains of *M. oryzae* infect different cultivars; *M. oryzae* 4091-5-8, the strain used in this research, infects barley. Blast epidemics on barley have been recorded in parts of Asia where barley grows close to rice [10]. While many resistance genes have been characterized in rice, only one resistance gene has been found in barley [10]. In comparison to other food crops, barley is less demanding in terms of its growing environments, therefore, the economic importance of the blast disease on barley has not been as devastating as that of rice [11]. However, as *M. oryzae* begins to shift host, as was apparent in wheat blast outbreaks in South America, the difficulty on farmers to increase the area and production of crops in this region has become a serious issue [12].

Magnaporthe oryzae has a fully sequenced genome making it a model organism for plant-pathogen interaction studies. The genome has been analyzed to identify key components involved in the adaptations needed for the fungus to cause disease in its host [4]. By isolating and studying the function of the genes, scientists have been able to identify over 40 avirulence genes [13]. The identification of these avirulence genes has been beneficial as disease resistant lines of rice have been

developed using this knowledge of targeting virulence factors [2]. Resistance builds once the pathogen is able to molecularly detect the avirulence factor targeting its persistence in the population. Selection pressures leads to a mutation in the fungus, allowing it to defeat plant resistance. The continuation of such molecular studies of plant-pathogen interactions are critical as fungicides are not always the most suitable option when natural resistance is overcome. As virulence is controlled by many genes, it is critical to understand its mechanistic basis in this fungus.

1.2 Gene Regulation by mRNA Degradation

An important part of gene regulation is mRNA degradation and the control of translation as cells transcribe more RNA than needed. The majority of RNA is degraded via three major pathways: by the exosome, through de-capping followed by 5'→3' exoribonuclease activity, or by the function of endonucleases. The exosome is a complex involving many proteins that degrade RNA from the 3'→5' direction [14]. In the de-capping with 5'→3' exoribonuclease activity, deadenylation, or shortening of the mRNA 3′ poly(A) tail, often occurs before de-capping [15]. This removal of the cap makes the RNA a preferred substrate to exoribonucleases, such as *XRN1* [14]. Within this research, I examine the role of *XRN1* in *Magnaporthe oryzae* as it pertains to mRNA degradation. Additionally, a subunit within the CCR4-NOT complex involved in deadenylase activity, *CAF16,* will also be studied.

1.2.1 *XRN1*

XRN1 in yeast was first purified and characterized by Audrey Stevens in 1978 [16]. Structurally, *XRN1* is highly conserved in N-terminal region of the protein, with sequence most conserved at the active site among XRN families [17]. Classified as a

5’→3’ exoribonuclease, studies in yeast have attributed the lack of this gene with significantly slowed growth, strongly suggesting that *XRN1* is involved in cell maintenance, specifically in mRNA turnover [18]. As well as degrading 5’ to 3’mRNA, *XRN1* can degrade a wide range of cytoplasmic RNA that are noncoding or targets for Nonsense Mediated Decay (NMD) [17]. Studies in Arabidopsis have suggested that the absence of an *XRN1* homolog, *XRN4*, led to an increase in gene silencing [19]. Without this exoribonuclease, it is suggested that there would be an accumulation of uncapped RNAs which would become substrates for RNA-Dependent RNA polymerase, leading to small interfering RNAs that become targets for degradation [14]. Deletion of *XRN1* has been observed to also cause defects in viability during nitrogen starvation, stagnant or ineffective meiotic processes, defective sporulation, telomere shortening, and chromosomal stability with no direct link to the deficiency of the *XRN1* activity [20]. XRN families are involved in ribosomal RNA maturation and transcription termination [17]. When switching to non-fermentable carbon sources, such as glycerol, *XRN1* is essential to the growth of yeast on that source [20].

In yeast, a scavenger de-capping enzyme, Dcs1, was shown to help facilitate the mechanisms and activity of *XRN1*. This enzyme enhances the affinity of *XRN1* to its target RNAs. To further develop our phenotypic analysis, we examined expression levels of *Dcs1* in the absence of *XRN1* to see if we could model the conclusions from the Sinturel et al, 2012 article. In addition, we also measured expression levels of *POR1*, a mitochondrial porin essential for mitochondrial respiration, as the same study observed a defect in the expression of this gene in *XRN1* mutants [20].

1.2.2 *CAF16*

A component in the CCR4-NOT complex, *CAF16* is a subunit associated with CCR4 [21]. The CCR4-NOT complex is a conserved multi-part complex involved in the regulation of gene expression. The core of the complex consists of CCR4, CAF1, and five NOT proteins [22]. Through electron microscopy, it was noted to have an L shaped, with 2 arms of similar length. Two enzymatic activities associated with the complex are deadenlyation and ubiquitination [23]. In ubiquitination, a protein is inactivated by attaching the small molecule of ubiquitin to it. This tags the protein and signals protein transport machinery to carry the protein to a proteasome for degradation [24]. Ubiquitination is associated with the NOT portion of the complex. Deadenylation, the poly(A) tail-shortening process, is provided by the CCR4 subunit. This shortening process is the first and rate-limiting step, and is also the most effective step in regulating mRNA degradation [25]. CCR4 has an exonuclease domain, and is a 3' exoribonuclease with a preference for poly (A) substrates. Caf1 bridges the CCR4 and NOT complexes together. Not only is this complex involved in degradation, but studies have shown its involvement in mRNA synthesis and translation thus proving to be a major contributor to gene expression [23].

1.3 Research/Objectives

Over time, researchers, our own labs included, have noted that samples of *M. oryzae* kept in the lab decrease in sporulation and begin to sector versus strains normally occurring in the field. Largely found as asexual spores in the field, it poses the question of how it retains successful persistence in the field, whereas lab strains seem to degrade. The factors of stress that are imposed often with lab strains can be indicative that in times of stress, there is decreased virulence as an adaptation to the

event. mRNA levels are regulated during times of stress, so it is possible that mRNA turnover is indicative of a global mechanism for gene regulation in the organism.

The importance of this research is in the concept of sustainability. Current control measures are often met with fungal resistance and increasing fungicide costs, thereby increasing costs to farmers and consumers. Our goal is to find sustainable solutions in the molecular mechanisms underlying pathogen virulence. Therefore, understanding microbe-plant interactions is a crucial component to sustaining control measures for pathogens that cause devastations of this magnitude. My research goal was to better understand the role of mRNA degradation in *M. oryzae*, and whether it contributed to virulence. The specific research objectives were to generate and analyze △*xrn1* and △*caf16* mutants in *M. oryzae* through molecular profiling of other genes, pathogenicity assays, and growth assays during stress conditions.

Chapter 2

PHENOTYPIC ANALYSIS BY GROWTH RATE ASSAYS IN MEDIA

2.1 Methods

2.1.1 Development of △*xrn1* and △*caf16*

For all experiments, we used *Magnaporthe oryzae* 4091-5-8, a barley-infecting strain, and was originally provided by the Sweigard Lab. To first isolate the *XRN1* gene, we used the available sequence of *XRN1* in yeast and performed a BLASTN search against the available *Magnaporthe oryzae* sequence from the Broad Institute, now accessible through the National Center for Biotechnology (NCBI) database. The search returned a sequence that was 44% homologous DNA sequence, 66% amino acid sequence to *XRN1* from yeast (MGG_12403.7) using the NCBI database. Using the sequence, we also extrapolated about 2,000 base pairs in 5' and 3' genomic flanking regions to assist with designing the deletion construct. To assist with primer and construct design, the software program, VECTOR NTI, was used and provided by the DuPont Labs. Primers were designed using a natural *Not*I site in the 5' flanking region of the *XRN1* gene (Primers EV15 & EV16). All primers used in this research are located on Table 2.1. Primer sequences were selected with G/C contents between 40-60% and melting temperatures of 55-66˚C. For the 3' flanking region, we added an artificial *Bam*HI site at the edge of the outer primer as there weren't any unique restriction sites in this region (Primers EV17 & EV18). This later assisted in the construction of a plasmid for amplification. For the purposes of detection, we used a Hygromycin B resistant (hygromycin B phosphotransferase, or *HPH*) to replace the *XRN1* sequence. Primers with overlapping complementarity to their corresponding flanking region were designed to help with the integration of *HPH*. To amplify the 5',

3’ flanking regions, and *HPH*, I used a PCR program set to 35 cycles, with an initial denaturation at 95°C for 10 seconds, 62°C for 15 seconds during annealing phase (based on primer melting temperatures), and 72°C for 2 minutes in the elongation phase. The PCR reaction was mixed according to the instructions for Q5® High Fidelity 2X Master Mix (New England BioLabs).

Once the fragments were amplified, they were run on a 1% gel using agarose gel electrophoresis to confirm we achieved the intended product. The three fragments were “zipped up” using the Gibson Assembly® method (New England Bio Labs). This final fragment was run on a 1% gel to confirm the intended product. The △*xrn1* fragment was then cut via restriction enzymes, *Not*I and *Bam*HI, and ligated to a plasmid, pSM563. The plasmid was then electroporated into a competent *Escherichia coli* cell line for cloning purposes. The culture was grown for a period of 24 hours in a shaking incubator (80 RPM, 37°C) before DNA was extracted. The plasmid DNA was verified using unique restriction sites *Pvu*I and *Pvu*II within the fragment and then sequenced (M13 Forward, M13 Reverse, and S2658, S2659, S2660, and S2661, Table 2.1). Primers EV45 and EV46 were used to excise any artificial sites and nucleotides to prepare for fungal transformation. The gene knockout design for *CAF16* (MGG_09520.7) was executed in the same manner as *XRN1*. *CAF16* in *M. oryzae* has a 56% and 72% homology to yeast genomic and amino acid sequences, respectively.

2.1.2 Fungal Transformation

We obtained *Magnaporthe oryzae* 4091-5-8 filter paper stocks from the Sweigard Lab and used it as a source to start wild-type controls throughout all experiments. Using previously made *Magnaporthe oryzae* 4091-5-8 protoplasts prepared using standard protocols in the Sweigard and Donofrio labs, we thawed the

cells at room temperature. In a Falcon 2059 tube, we mixed 140µl of the protoplasts cell volume with 20µl of the DNA that contained the confirmed knockout gene *(⊿xrn1 and ⊿caf16).* Mixture was incubated at room temperature for 15 minutes. One milliliter of PTC (40% PEG 3350 in STC (20% sucrose, 50mM Tris-Cl, pH 8.0, and 50mM $CaCl_2$) was added and gently mixed to not destroy the protoplasts. Room temperature incubation followed for 20 minutes. Five milliliters of TB3 (For 1 liter: 3g yeast extract, 3g casamino acids, and 20% sucrose) were added to the mixture and incubated at room temperature on a shaker for a 4-hour period. Cells were pelleted and re-suspended using TB3. Molten top agarose (40°C -44°C) was added to the re-suspended cells and mixed thoroughly. The mixture was then poured onto bottom agar evenly. Transformants were collected on Day 5 post-transformation. Mutants were then isolated and single spored onto complete media with Hygromycin selection. Micro-centrifuge tubes containing 0.5mm silica beads (bead beater tubes) and 100µl of liquid complete were used to culture extracted samples for the transformant screen. The cultures were grown for two days followed by the addition of DNA extraction buffer (1X phosphate buffered saline (PBS) with 0.1% sodium dodecyl sulfate (SDS). The bead beater tubes were vigorously shaken for 30 seconds to macerate the culture. Qiagen DNA extraction columns (Qiagen, MD, USA) were used to isolate genomic DNA; genomic DNA was isolated for PCR use. To test the presence of the entire fragment, primers EV47 and EV50 were designed outside of the fragment, about 1.2kb away from fragment on 5' flanking region and about 1kb away from the 3' flanking region end. For the 5' side of this construct, a set of primers was designed to read from the outside of the Δ*xrn1* fragment using the previous primer EV47 and then out of the *HPH* center-piece (EV58). For the 3' side of this construct, a primer was designed to

read from the *HPH* center-piece (EV57) to the outside of the △*xrn1* fragment using the previous primer EV50. PCR products were then run on a 1% gel using agarose gel electrophoresis to confirm mutants from the transformation. Two independently transformed lines from each deletion construct were selected and confirmed for use in further studies. To confidently attribute a phenotype to the loss of a gene, we performed complementation studies, re-inserting the deleted gene back into its corresponding mutant line. To accomplish this, we used the sequence in the 5' and 3' flanking regions to design a native promoter and terminator. This gene with its native promoter and terminator was ligated to plasmid, pFU47 and then transformed into the mutant protoplasts. All mutants were made into protoplasts using the Parsons et. al, 1987 method with the exception of protoplasts were released enzymatically using Novozym 234 (Sigma Lysing enzyme Catalog number L-1412)/Chitinase/B-D-glucanase Solution [26].

2.1.3 Growth Rate Assays

All mutants and wild-type strains were maintained at 25°C under constant fluorescent light. In the first growth rate assay, we used complete media (CM 1 liter: 10g sucrose, 6g yeast extract, 6g casamino acid, 1ml trace element, 12g agar), oatmeal agar (OA 1 liter: 50g granulated oatmeal, 15g agar), minimal media (MM, 1 liter:10g sucrose, 1ml trace element, 50ml 20x nitrates, 1mg of thiamin, 5μg of biotin, 15g agar), and Reactive Oxygen Species media with H_2O_2 (ROS, 1 liter, 10g sucrose, 6g casamino acids, 6g yeast, 1ml trace elements, 15g agar, and 10ml of 3% hydrogen peroxide added at cooling of media). All media was prepared using aseptic technique and autoclaved. Six millimeter punches of the mutants (grown on complete media) were placed on the media mentioned. Their growth rates were measured daily with a

centimeter ruler at the same time every day, marking on the plate the outermost growth made by the organism in the media for that day. We took measurements beginning on Day 5 post inoculation, and captured images on Day 7.

Another set of varying media types was used for further phenotypic analysis. We used malt yeast agar media (MYE, 1 liter: 14g malt, 2g yeast, 15g agar) and nitrogen starved media (NS: 1 liter, 0.5g Potassium Chloride, 0.5g Magnesium Sulfate, 1.5 Potassium Phosphate, 10g glucose, and 1ml trace elements). We also introduced a different reactive oxygen species, Paraquat (Sigma-Aldrich), and used it at a 10μM and 100μM concentrations. This compound, which catalyzes a superoxide free radical, was added at cooling of media post-autoclave (For 1 liter: 24g Potato Dextrose Broth, 12g Agar). Complete media was prepared to serve as the control.

To understand the growth rates and morphology during hyperosmotic stress, glycerol and sorbitol media were used. We prepared a 10% glycerol media that contained all the ingredients for a 1 liter complete media recipe except for sucrose. In lieu of sucrose, we used glycerol. For the sorbitol media recipe, we also followed the recipe for complete media and instead of sucrose, we used sorbitol for a final concentration of 1M.

2.2 Results

2.2.1 Development of △*xrn1* and △*caf16*

2.2.1.1 Development of △*xrn1*

To generate the *XRN1* mutant, we used the NCBI database to determine the homologous gene to yeast for *XRN1*. The *XRN1* gene was determined to be 4.3kb in length (Figure 2.1A). Using the natural *Not*1 restriction sites (120 base pairs in from

the outer edge primer (EV15)), and primer EV16, the 5' flanking region was 1,725 base pairs in length. For the 3' flanking region, primer EV17 and primer EV18 with the artificial *Bam*HI restriction site within the primer sequence, was determined to be 1,260 base pairs in length (Figure 2.1A). Using primers EV19 and EV20, *HPH* was 1.4 kb in length with an approximate 20 nucleotides overlap with its corresponding flanking region (Figure 2.1B). Figure 2.2A indicates the PCR products on a 1% gel confirming the three separate fragments prior to Gibson assembly. After the Gibson assembly, primers EV15 and EV18 were used to show the final △*xrn1* fragment at 4.4kb in length (Figure 2.2B). The △*xrn1* fragment was then cut with restriction enzymes *Not*I and *Bam*HI (expected band size: 4.3kb) and ligated to pSM563 (pBluSKP) (expected band size: 2.9kb) (Figure 2.3A). Vector NTI software was used to generate an image on the orientation of the plasmid with the knockout fragment introduced as well as the primer placement (Figure 2.3B). Using primers M13 Forward and M13 Reverse, as well as *HPH* primers, the plasmid was sequenced through each flanking region into the *HPH* centerpiece for full confirmation of proper gene knockout orientation. The plasmid was electroporated into an *E. Coli* Top 10 competent cell line (ThermoFisher Scientific). Once the DNA was extracted from the *E. coli* culture, *Pvu*I and *Pvu*II restriction enzymes were used to confirm positive clones (Figure 2.4). Confirmed clones were used to excise the final fragment via PCR, primers EV45 & EV46. Final fragment size was 3.8 kb (Figure 2.3C). To ensure primers for transformation worked, using Vector NTI images for primer placement (Figure 2.5A), we tested *HPH* primers EV51 & EV52 to produce a 1.4kb band size (Figure 2.5C). We then tested primers that went beyond the *HPH* gene to the outer flanking regions to produce 2.3kb PCR products on both sides (Figure 2.5B & 2.5D).

Finally, we tested primers (EV47 & EV50) that went from 5' flanking region through *HPH* to the 3' flanking region to produce a 6kb PCR product on the gel (Figure 2.5B &2.5D).

2.2.2 Complementation of *△xrn1*

To complement the mutants as an experimental control, we inserted the *XRN1* sequence to *△xrn1-14*. We used the previously acquired sequences from the 5' and 3' flanking regions to design the gene with its native promoter. Primer EV70 was designed with *Bam*HI site 489 base pairs from the start codon of the gene. Primer EV71 contains the *XRN1* terminator with *Xba*I site 291 base pairs from the stop codon. Primers EV70 and EV71 generated a 5,301-base pair long fragment with native promoter and terminator. This fragment was then ligated into plasmid pFU47, containing resistance marker, Bialophos, through T4 ligase. The *XRN1* plasmid was then transformed, as previously mentioned, into the mutant protoplasts that were generated. Transformants were then plated on Bialophos selection complete media and screened using primers EV70 and EV71. When screening for *XRN1*, a mutant was generated that lacked *XRN1* but has both *HPH* and Bialophos selection. We termed this mutant *△xrn1-16*, but should be noted that it is *△xrn1-14*, but with two section markers integrated into its genome.

2.2.2.1 Development of *△caf16*

To generate the *CAF16* mutant for our assays, we used the NCBI database to find the homologous to yeast sequence for *CAF16*. The *CAF16* gene is 987bp in length (Figure 2.7A). The 5' flanking region (primers EV27 and EV28) was 1.7kb base pairs in length with an artificial *Bam*HI restriction added by sequence into primer

EV27. For the 3’ flanking region, primer EV29 and primer EV30 was determined to be 1,260 base pairs in length (Figure 2.7A). Using primers EV31 and EV32, the Hygromycin R gene was 1.4 kb in length with an approximate 20 nucleotides overlap with its corresponding flanking region (Figure 2.7B). The Δ*caf16* fragment was then cut with restriction enzymes *Eco*RI (a blunt restriction site cutter) and *Bam*HI (expected band size: 4.3kb) and ligated to pSM563 (pBluSKP) (expected band size: 2.9kb) as a *Bam*/blunt ligation (Figure 2.8A& 2.8B). Using primers M13 Forward and M13 Reverse, as well as *HPH* primers, the plasmid was sequenced through each flanking region into the *HPH* centerpiece for full confirmation of the orientation of the knockout piece.

Once the DNA was extracted from the *E. coli* cell-line it was electroporated into, *Pvu*I, *Pvu*II, and *Aat*II restriction enzymes were used to confirm clones (Figure 2.9). The final fragment was excised from the confirmed clones via PCR, using primers EV43 & EV44. Final fragment for transformation was 4.0 kb (Figure 2.8C). To ensure primers for transformation worked, using Vector NTI images for primer placement (Figure 2.10A), we tested primers that went from the 5’ flanking region through *HPH* to the 3’ flanking region (EV59 & EV60) to produce a 5kb PCR product on the gel (Figure 2.10B).

2.2.3 Fungal Transformation of △*xrn1* and △*caf16*

In order to develop fungal mutants for the in vitro and in planta assays, a series of PCRs were conducted. Primers EV57 and EV58 (which had placement in the *HPH* and outward of the gene) were designed for the screening of mutants after transformation in addition to the outer edge primers EV47 and EV50 for △*xrn1* confirmation. Figure 2.6A, B, and C show a series of confirmatory gels using the PCR

products to screen and confirm △*xrn1* mutants. The △*xrn1* had two confirmed mutants that are termed at ⊿*xrn1*-9 and ⊿*xrn1*-14 for the duration of this research. Primers EV57 & EV58 were also used for the screening △*caf16* mutants which read inside and out of the *HPH* and were coupled with primers EV59 & EV60 to produce a 2.4kb PCR product (5' to *HPH*) and 1.8kb PCR product (*HPH* to 3') (Figure 2.11A & 2.11B) Screens revealed two mutants that are termed ⊿*caf16*-11 and ⊿*caf16*-19 for the duration of this research. *CAF16*-15 was also used in the assays as it showed evidence of ectopic integration of the *HPH* through selected media growth but no confirmed PCR using the primers for ⊿*caf16* mutants. This ectopic mutant will serve as an additional control that should be comparable to wild-type. Further confirmatory PCRs and gels were conducted to conclude △*caf16*-11 and △*caf16*-19 as true knockouts (Figure 2.12A, 2.12B, & 2.12C).

2.2.4 Growth Rate Assays

To determine if there are growth rate differences in selected stress media, we conducted a series of assays to assess this. Growth rates in the ROS (H_2O_2) media were all relative to wild-type in the 4 days measured (Figure 2.13). Minimal media, oatmeal media, and complete media growth rates were also relative to wild-type (Figures 2.14, 2.15, 2.16, respectively). Images were taken from the assays that contained varying concentrations of Paraquat (ROS), nitrogen starved conditions, and complete media (Figure 2.17 & 2.18). Growth rates for complete media remained relative to wild-type when the assay was repeated on a later date (Figure 2.19). Nitrogen starved media △*caf16* mutants stopped growing after Day 6 while the remaining mutants and wild-type continued to grow (Figure 2.20). The lower concentration of Paraquat 10uM (ROS) media had similar growth rates to wild-type

(Figure 2.21). When we increased the concentration of ROS (100uM), we saw faster rates in the mutants to wild-type and a slower rate from the ectopic, *CAF16*-EM (Figure 2.22). To visualize the morphology of the colonies produced by the mutants and wild-type, images were taken on Day 5 post inoculation for the assay where we tested two different hyperosmotic stressors, glycerol and sorbitol (Figure 2.23). For 1M sorbitol, growth rates were comparable to wild-type while the ectopic mutant, *CAF16*-EM had a slower growth rate than wild-type (Figure 2.24). In 10% glycerol growth conditions, we see a faster growth rate in the mutants in comparison to wild-type. The ectopic mutant, *CAF16*-EM was relative to wild-type. Due to contamination in the second set, values shown are based on one technical replicate for the 10% glycerol and 1M sorbitol assays.

Table 2.1 Primers Used in This Research

ID	**Tube Identification**	**Primer Sequence**	**Tm (°C)**	***Note*s**
UBC-F	*UBC*-FOR	CCGACGATGAAATTCCTAGGCGAA	59	Housekeeping gene used for qPCR
UBC-R	*UBC*-REV	ATGCGTGTTCGTAGTGGTGGG	59.9	Housekeeping gene used for qPCR
GAPDH-F	*GAPDH*f	TTGTCTTCCGCAATGCTATCGAGC	59.6	Housekeeping gene used for qPCR
GAPDH-R	*GAPDH*r	ACTTGACCTTCTTGCCGTTGACGA	60.7	Housekeeping gene used for qPCR
M13 F	M13 Forward	TGTAAAACGACGGCCAGT		Primers for plasmid sequencing
M13 R	M13 Reverse	GGAAACAGCTATGACCATG		Primers for plasmid sequencing
S2658	HygRout5a	TGTCGAACTTTTCGATCAG		sequence out from the 5' end of HygR 39 bp from ATG
S2659	HygRout5b	CCTACATCGAAGCTGAAAG		sequence out from the 5' end of HygR 103 bp from ATG
S2660	HygRout3a	TCGATGATGCAGCTTGG		sequence out from the 3' end of HygR 159 bp from termination codon

Table 2.1 Primers Used in This Research (Continued)

S2661	HygRout3b	CGATGGCTGTGTAGAAG		sequence out from the 3' end of HygR, 53 bp from termination codon
XRN1 -F	*XRN1*-F	TTGGTTCTACAAGTTCCACTACTC		*XRN1* FOR (RNA STUDY)
XRN1 -R	*XRN1*-R	GGTCTGGAAGAACACCCATAAG		*XRN1* REV (RNA STUDY)
XRN1 -F2	*XRN1*-F2	AGCGATTCATCGAGCGAGCC		*XRN1* For 2 (RNA)
XRN1 -R2	*XRN1*-R2	TTGGCAACGGCATAGGACGG		*XRN1* Rev 2 (RNA)
CAF16-F1	*CAF16*-F1	TGGTCGAGGTGCTGGACATT		*CAF16* FOR (RNA study)
CAF16-R1	*CAF16*-R1	CAGGTTGTCGAGAATGTGGGT		*CAF16* REV (RNA study)
CAF16-F2	*CAF16*-F2	ATCGTGCGCACCGACATT		*CAF16* FOR (2)
CAF16-R2	*CAF16*-R2	AACGAGACAGCACGTCGAG		*CAF16* REV (2)
CAF16-F3	*CAF16*-F3	TGACGTACAGCTTTCCAGACCG		Caf16 For (3)
CAF16-R3	*CAF16*-R3	GTTCAGCACCCACTCCAGCC		Caf16 Rev (3)
CAF16-F4	*CAF16*-F4	AGCAACATCAGTCTTTCGCTGC		Caf16 For (4) (Rev is Caf16 Rev 3)
CAF16-F5	*CAF16*-F5	CTCGTT CGGGCTTCCTCGAC		Caf16 For 5
CAF16-R5	*CAF16*-R5	CTTGAGGTCTTCCCGCAGCC		Caf16 Rev 5
EV1	>12403 5’ FOR	CCTGGTCAAAGTCTTCCTCTAC	65	*XRN1* primers not used in this study
EV2	>12403 5’ REV	CACGGCGCGCCTAGCAGCGGGTCG ACTAGATCCGTCTTCAAC	-	*XRN1* primers not used in this study
EV3	>12403 3’ FOR	GCAGGGATGCGGCCGCTGACAGCG GGAATGGTTTACGAATAA	-	*XRN1* primers not used in this study
EV4	>12403 3’REV	GCACTACTACAGCAGCAAGAA	66	*XRN1* primers not used in this study
EV5	>12403 3’ FOR2	GCAGGGATGCGGCCGCTGACAACA TGGGTGGTCGAGGT	-	*XRN1* primers not used in this study
EV6	>12403 3’ REV2	CGCTCAAGAAGCTGAAGAAGAG	66	*XRN1* primers not used in this study
EV7	>*HPH*F	CCGCTGCTAGGCGCGCCGTGGCTG GAGCTAGTGGAGGTCA	-	*HPH* primers
EV8	>*HPH*R	GTCAGCGGCCGCATCCCTGCGGTC GGCATCTACTCTATTC	-	*HPH* primers
EV9	12403*XRN1*3' FOR	GCAGGGATGCGGCCGCTGACGTTG GGTGTTTGGTACAGAGAG	-	Primers with overlap to Hyg
EV10	12403*XRN1*3' REV	CGTCTATCGCCATGAAGAACAA	66	Primers with overlap to Hyg
EV11	09520 *CAF16* 5'FOR	GGTGGCCAGTACAACATCTATC	66	*CAF16* primers not used in this study
EV12	09520 *CAF16* 5'REV	CACGGCGCGCCTAGCAGCGGGGCC TTACAGGATACAAGCAA	-	*CAF16* primers not used in this study

Table 2.1 Primers Used in This Research (Continued)

EV13	09520 *CAF16* 3' FOR	GCAGGGATGCGGCCGCTGACGCCG GTCTTATGGGTGATATT	-	*CAF16* primers not used in this study
EV14	09520 *CAF16* 3' REV	TCTTCGCTGAATACTTGGTACTT	64	*CAF16* primers not used in this study
EV15	Xrn1-5'-For	GCCGTCGCTATGATATCAG	64	1725 bp product; natural *Not* I site downstream makes ~1600 bp frag
EV16	Xrn1-5'-rev	CAATATCAGTTAACGTCGACGAAT AAGGTCTTGGCAGTTATAGC	61	
EV17	Xrn1-3'-For	GAACCAGTTAACGTCGACGAATGA TGGCGTGTCGTGATAG	61	1260 bp product
EV18	Xrn1-3'-rev	TTTTTTTT**GGATCC**CAGCAAGAAG GAGGAGTAC	62	has *Bam* site
EV19	HygFor-Xrn	GCTATAACTGCCAAGACCTTATTC GTCGACGTTAACTGATATTG	61	Overlap is underlined
EV20	HygRev-Xrn	CTATCACGACACGCCATCATTCGT CGACGTTAACTGGTTC	64	Overlap is underlined
EV21	Caf16-5'-For	AAAAAA**GGATCC**ATGAAGCTACA GTCGGATTTG	61	1364 bp frag, has ***Bam*HI site**; Wrong orientation Gene
EV22	Caf16-5'-Rev	CAATATCAGTTAACGTCGACGAAT CTCAGACTCGTTGAGTGCAG	64	Wrong orientation Gene
EV23	Caf16-3' For	GAACCAGTTAACGTCGACGAATAG TTGCGGTGATTCTGC	62	Wrong orientation Gene
EV24	Caf16-3' Rev	TTTTTT**GCGGCCGC**GCTCCGGTGC TATATAATCC	61	1449 bg frag, has ***Not*I site**; Wrong orientation Gene
EV25	HygFor-Caf16	CTGCACTCAACGAGTCTGAGATTC GTCGACGTTAACTGATATTG	61	Wrong orientation Gene
EV26	HygRev-Caf16	GCAGAATCACCGCAACTATTCGTC GACGTTAACTGGTTC	64	Wrong orientation Gene
EV27	Caf16-5'-For	AAAAAA**GGATCC**CATTCAGGCAA GAACTCCTAAAC	62	1709 bp frag, *Bam*HI site
EV28	Caf16-5'-Rev	CAATATCAGTTAACGTCGACGAAT GCATCCACATTATTCGCTGATAC	63	Overlap is underlined
EV29	Caf16-3' For	GAACCAGTTAACGTCGACGAATCC GGTCTTATGGGTGATATTTG	62	Overlap is underlined
EV30	Caf16-3' Rev	TTTTTTGCGGCCGCCTGGAACGGT AAGGATAGGATAG	63	1297 bp frag, *Not*I site
EV31	HygFor-Caf16	GTATCAGCGAATAATGTGGATGCA TTCGTCGACGTTAACTGATATTG	61	Overlap is underlined
EV32	HygRev-Caf16	CAAATATCACCCATAAGACCGGAT TCGTCGACGTTAACTGGTTC	64	Overlap is underlined
EV33	HygFor-XrnB	TCTTCGCTATAACTGCCAAGACCTT ATTCGTCGACGTTAACTGATATTG		longer version of EV19 with more overlap
EV34	HygRev-XrnB	CCCCAGTCACTATCACGACACGCC ATCATTCGTCGACGTTAACTGGTTC		longer version of EV20 with more overlap
EV35	HygR-For	AGAATCTCGTGCTTTCAGCTTC	64	Forward in HygR, 107 bp overlap with EV35
EV36	HygR-Rev	CAAAGTGCCGATAAACATAACGAT C	63	reverse in HygR
EV37	Caf16-5'-ForShort	AAAAGGATCCCATTCAGGCAAG	64	Shorter flanking regions
EV38	Caf16-3' Revshort	GCCTGGAACGGTAAGGATAG	64	Shorter flanking regions

Table 2.1 Primers Used in This Research (Continued)

EV39	Xrn1-5'-ForShort	CTGGGTGATGTTCCACTTGATAG	64	Shorter flanking regions
EV40	Xrn1-3'-revshort	TTTTTGGATCCCAGCAAGAAGG	64	Shorter flanking regions
EV41	Xrn1-5'-ForShorter	AGTCTTCCTCTACGTCCATTTC	63	makes 1163 bp fragment
EV42	Caf16-5'-ForShorter	TTGATGACCATGCTCATCAAGTAC	64	makes 1195 bp fragment
EV43	*CAF16*KO5	GCCTGGAACGGTAAGGATAG	64	
EV44	*CAF16*K03	GGGTGGTGAAGCTATATACG	61	makes a 4005 bp fragment
EV45	*XRN1*KO5	AGCAAGAAGGAGGAGTACG	63	
EV46	*XRN1*KO3	TGAGAAACGGATGAACAGC	61	makes a 3800 bp fragment
EV47	*XRN1*-FT 5' for	GCATCATCTGGTTGTTGCTC	63	
EV48	*XRN1*-FT 5' rev	GTCTTGGCAGTTATAGCGAAG	62	makes a 2.3 kb fragment
EV49	*XRN1*-FT 3' for	ATGGCGTGTCGTGATAGTG	64	
EV50	*XRN1*-FT 3' rev	GCTATCCAGATAATCGCGAC	62	makes a 2.3 kb fragment
EV51	HYG-FT for	ATTCGTCGACGTTAACTGATATTG	61	
EV52	HYG-FT rev	ATTCGTCGACGTTAACTGGTTC	64	makes a 1.4 kb fragment
EV53	*CAF16*-FT 5' for	CATTCAGGCAAGAACTCCTAAAC	62	
EV54	*CAF16*-FT 5' rev	GCATCCACATTATTCGCTGATAC	63	makes a 1.7 kb fragment
EV55	*CAF16*-FT 3' for	CCGGTCTTATGGGTGATATTTG	62	
EV56	*CAF16*-FT 3' rev	GGATGAGATTGACAGTGCG	62	makes a 1.6 kb fragment
EV57	HYG-F	GTTGGCTTGTATGGAGCAG	62	
EV58	HYG-R	CAGAAACTTCTCGACAGACGTC	64	
EV59	*CAF16*-4091 FOR	TCTCTTCTTGCAACGGCTTG	64	
EV60	*CAF16*-4091 REV	CATTAGTGACGCCGAGGAGA	65	makes a 5kb fragment
EV61	*CAF16*-4091 FOR2	GCCTCGGACATAAGTGTGTG	65	
EV62	*CAF16*-4091 REV2	GATCTTTGTGCTGGCGGTGA	67	makes a 5.7kb fragment
EV63	*XRN1*-5' FOR MC	CTGCCTTGTGTCAAGAATCTGC	65	
EV64	*XRN1*-HYG-3' REV MC	CGAACTTAAGAAGGTATGACCG	62	makes a 2.3 kb fragment
EV65	*XRN1*-5' FOR MC	GCTTCAGGATACGGTTGTTG	62	
EV66	*XRN1*-HYG-3' REV MC2	GAGATGCAATAGGTCAGGCT	63	makes 2.8 kb fragment

Table 2.1 Primers Used in This Research (Continued)

EV67	*XRN1*-5' FOR MC2	GCTCCTGGTCAAAGTCTTC	61	
EV68	*XRN1*-5' FOR MC3	ACCAAGTCAGCAACTAAAGC	61	
EV69	*XRN1*-5' FOR MC4	GGGTTTTGAGGCTGGTATC	61	outside cloned region
EV70	*XRN1* for Complement F	ACACCCAACCtctagataacactctagtgcttcc	62	reverse in Mg *XRN1* terminator with Xba site 291 bp from STOP
EV71	*XRN1* for Complement R	GAGTCAAAAG**GGATCC**ACCGATG ACTGTCATTTAG	64	forward in *XRN1* promoter with *Bam*H I site 489 bp from ATG; 5301 bp
EV72	EV-*DCS1*-1F	GCACGTTGAATCAAGACCAAGC	55	Around intron
EV73	EV-*DCS1*-2R	GTCACGGAGGAGAGGTAGTC	53	Makes 128 bp PCR product
EV74	EV-*DCS1*-3F	CTGCTCCCAGACCTGAACTG	56	
EV75	EV-*DCS1*-4R	CAATCTCGGGGTACACCTCG	56	Makes 175 bp PCR product
EV76	EV-*DCS1*-5F	GCCGACGTACTACCACTTCC	54	
EV77	EV-*DCS1*-6R	ATTTCGGTCCACAACTCGCT	54	Makes 198 bp PCR product
EV78	EV-*DCS1*-7F	CCGAGATTGAGCGGGATCAG	56	
EV79	EV-*DCS1*-8R	CGTGCACGATGTGTATGTGG	54	Makes 81 bp PCR product
EV80	EV-*POR1*-9F	CAACGACTTGCTCACCAGGG	55	Around intron
EV81	EV-*POR1*-10R	GTCAGGCCGAGAGACTTGTC	54	Around intron, 168 bp PCR product
EV82	EV-*POR1*-11F	GACAAGTCTCTCGGCCTGAC	54	Around intron
EV83	EV-*POR1*-12R	CTGCTTGAAGTGCAGGTT AG	55	Make 171bp PCR product
EV84	EV-*POR1*-13F	CGCTGCCAGCTATTACCACA	56	
EV85	EV-*POR1*-14R	CTTGCCCTTGACGAAGGACAG	56	Around intron, 142 bp PCR product
EV86	EV-*POR1*-15F	CTGAACCTGCACTTCAAGCAG	56	
EV87	EV-*POR1*-16R	CTTCTGGACGTTGTAGCCACC	55	Make 76bp PCR product

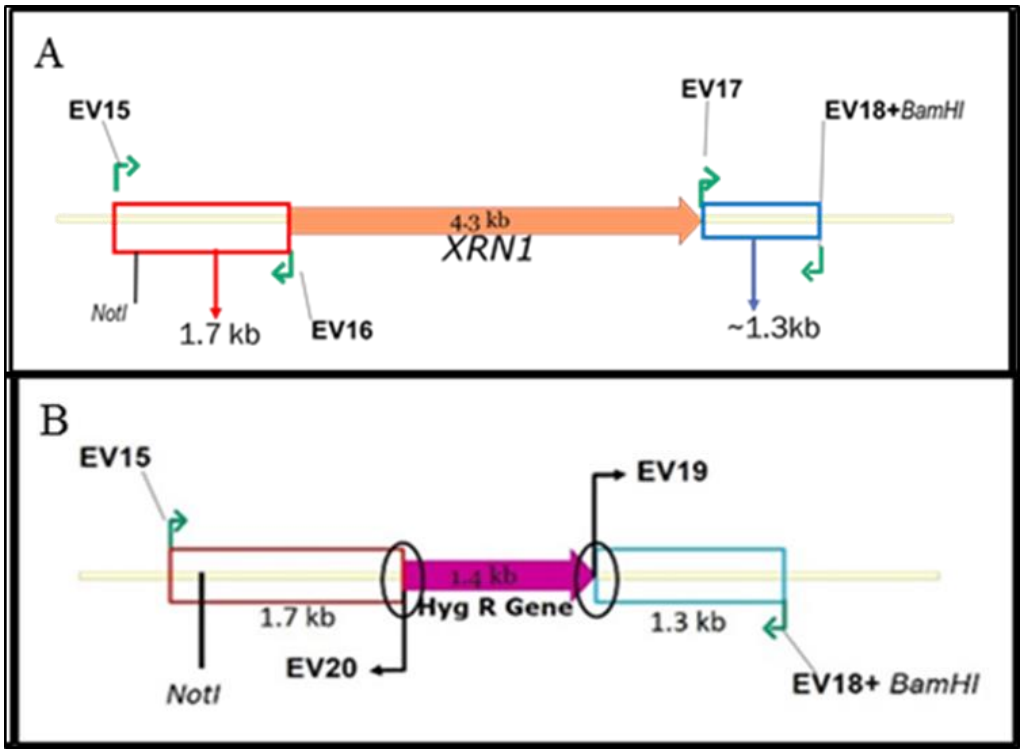

Figure 2.1 Graphic Representation of *XRN1* and △*xrn1*. A. Graphical representation of the *XRN1* gene, 5' and 3' flanking regions. This illustration shows the placement of the primers in the flanking regions as well as the representation of length for *XRN1* gene. Natural *Not*I site and artificial *Bam*HI restriction site (added by primer) also depicted. B. Graphical representation of the △*xrn1* with the placement of primers EV19 and EV20 circled for representation of ~20 nucleotide overlap.

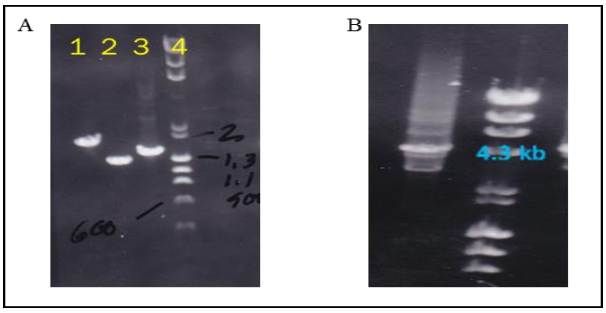

Figure 2.2 Images from gel electrophoresis using a 1% agarose gel with Ethidium Bromide. A. From lanes left to right: 1. *XRN1*-5' Flanking Region - 1.7kb; 2. *XRN1*-3' Flanking Region-~1.3kb; 3. *HPH*-1.4kb; 4. Lambda *Hind*III/*Hae* III Marker. B. Image from gel electrophoresis using a 1% agarose gel with Ethidium Bromide. Left lane, Gibson Assembly Fragment, △*xrn1*-4.4kb. Right lane, Lambda *Hind*III/*Hae* III Marker.

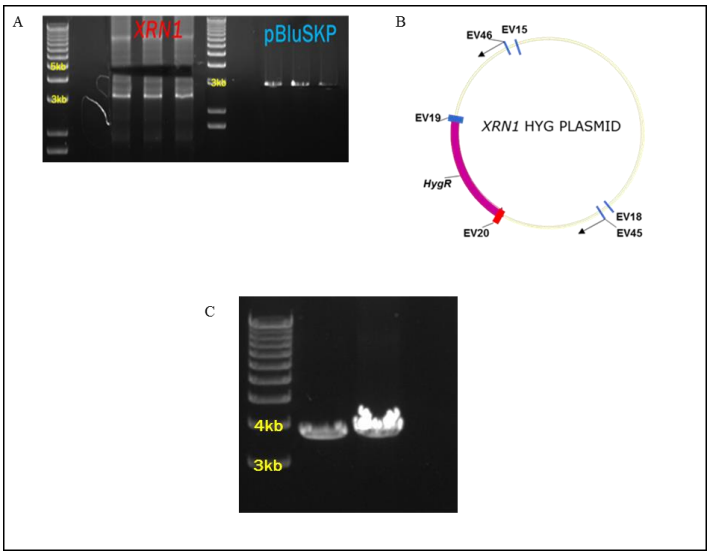

Figure 2.3 Plasmid Creation for △*xrn1*. A. Gel electrophoresis picture provides evidence of the restriction enzyme cut fragment from △*xrn1* and pSM563 (pBluSKP) that were used for purification and ligation. △*xrn1* was cut at 4.3kb and the plasmid was cut at 2.9kb. B. Graphical representation of the plasmid that was created after the fragments mentioned previously were ligated. Illustration also shows the primer placement for the final fragment that was used for fungal transformation (EV45 & EV46). C. Gel electrophoresis image from the PCR product created using primers EV45 & EV46, product size 3.8kb.

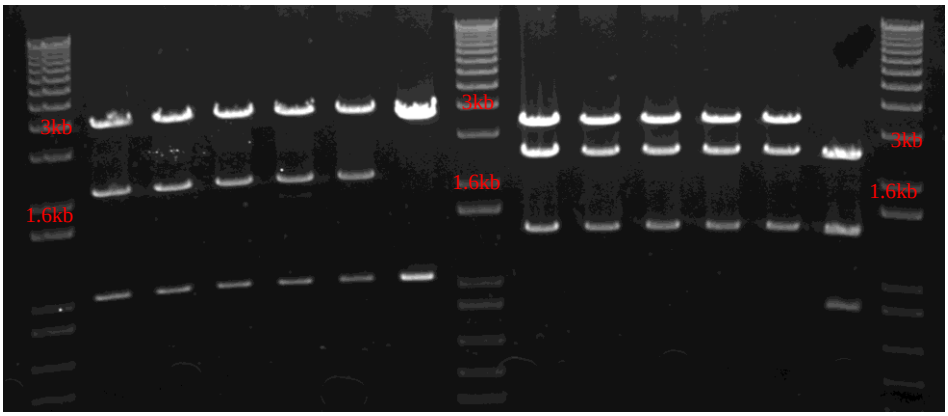

Figure 2.4 Diagnostic Restriction Enzyme Digest to Confirm △*xrn1*plasmid fragment using *Pvu*I, *Pvu*II, and *Aat*II cutters. Lane 1, 8, and 15 were 1Kb+ Markers. Lanes 2-7 were ⊿*xrn1* plasmid DNA cut with *Pvu*I-Expected bands: 4037bp, 2182bp, 1045bp. Lanes 9-14 were ⊿*xrn1* plasmid DNA cut with *Pvu*II-Expected bands: 3329bp, 2513bp, 1422bp.

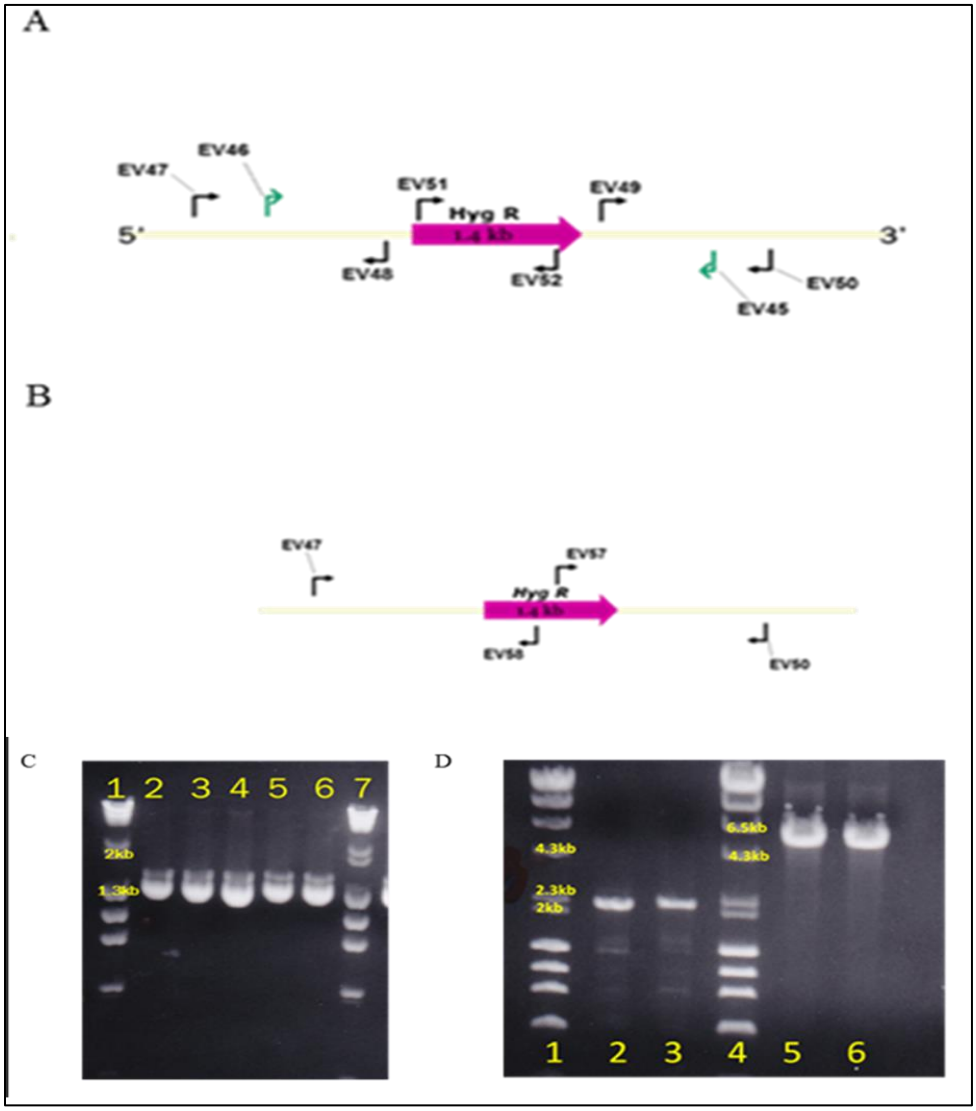

Figure 2.5 Confirmation of ⧋*xrn1* through PCR. A. Graphical representation (Vector NTI) of the ⧋*xrn1* vector design with primer placement, emphasis on the *HPH* primers. B. Graphical representation of ⧋*xrn1* with emphasis on the primer placement to produce two PCR products that won't be found elsewhere in the genome. C. Gel electrophoresis image from PCR product of the *HPH* primers, EV51 & EV52, expected product 1.4kb. Five replicates shown, Lambda *Hind*III/*Hae*II Marker used in lanes 1 & 7. D. Gel electrophoresis image showing PCR products from primers EV47 & EV48 (Lanes 2), expected product 2.3kb, primers EV49 & EV50 (Lane 3), expected products 2.3kb. Primers EV 47 & EV50 produce a 6kb fragment (Lane 5&6). Lambda *Hind*III/*Hae*II Marker used in lanes 1 & 4.

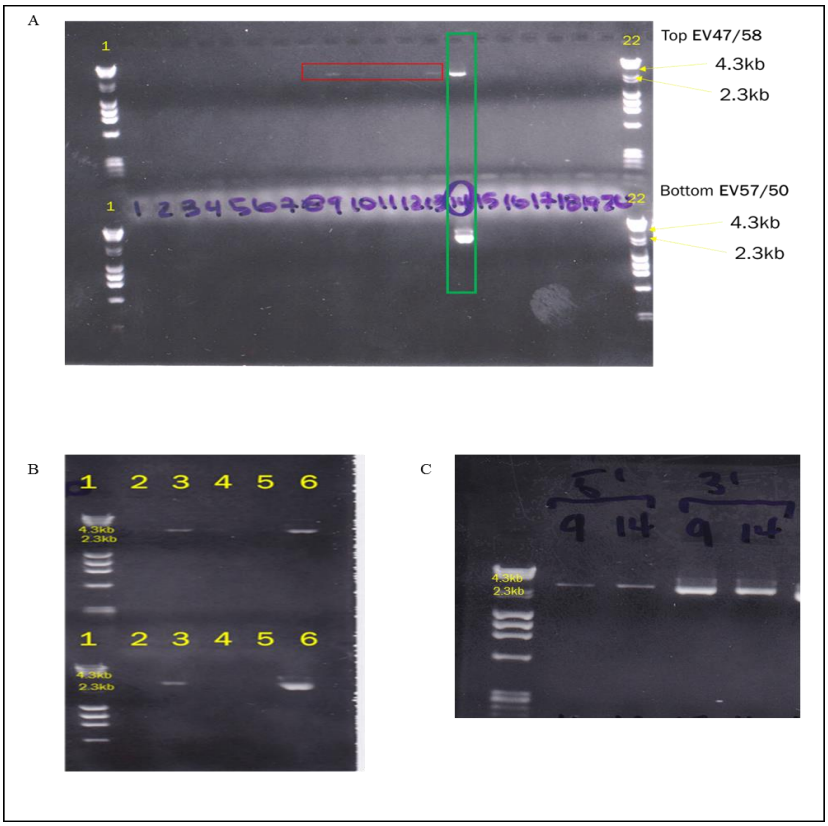

Figure 2.6 △*xrn1* Fungal Transformation Confirmatory PCR Products on Gel Electrophoresis. A. Gel electrophoresis image showing PCR products from a screen of 20 transformants from the fungal transformation. Lanes 1 & 22 Lambda *Hind*III/*Hae*II Marker. For the 5' side of this construct, a set of primers was designed to read from the outside of the △*xrn1* fragment using the previous primer EV47 and then out of the Hyg center-piece, primer EV58. Fragment is 2785 bp in length. For the 3' side of this construct, a primer was designed to read from the Hyg center-piece, primer EV57 to the outside of the △*xrn1* fragment using the previous primer EV50. Fragment is 2691 bp in length. B. Top: Lane 1-Lambda *Hind*III/*Hae* Marker, Lane 2-△*xrn1* Transformant 1 -5, Lane 3-△*xrn1* Transformant 9 -5', Lane 4-△*xrn1* Transformant 10 -5', Lane 5-△*xrn1* Transformant 13 -5', Lane 6-△*xrn1* Transformant 14 -5'. Bottom: Lane 1-Lambda *Hind*III/*Hae* Marker, Lane 2-△*xrn1* Transformant 1 -3', Lane 3-△*xrn1* Transformant 9 -3', Lane 4-△*xrn1* Transformant 10 -3', Lane 5-△*xrn1* Transformant 13 -3', Lane 6-△*xrn1* Transformant 14 -3'. C. Gel electrophoresis image using transformant 9 & 14 for further confirmation by PCR. Lane 1-Lambda *Hind*III/*Hae* Marker, Lane 2-△*xrn1* Transformant 9 -5', Lane 3-△*xrn1* Transformant 14 -5', Lane 4-△*xrn1* Transformant 9 -3', Lane 5-△*xrn1* Transformant 14 -3'.

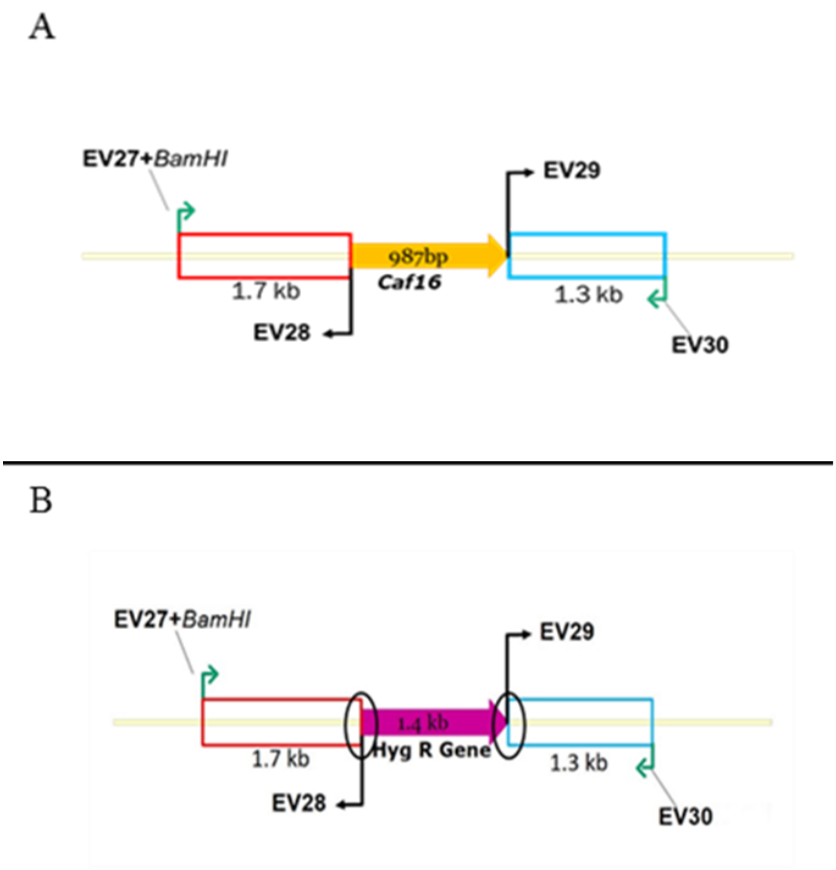

Figure 2.7 *CAF16* Gene with Flanking Regions and △*caf16* Development. A. Graphical representation (Vector NTI) of *CAF16* showing the primer placement for development of the 5' and 3' flanking regions. B. Graphical representation (Vector NTI) of the △*caf16* fragment.

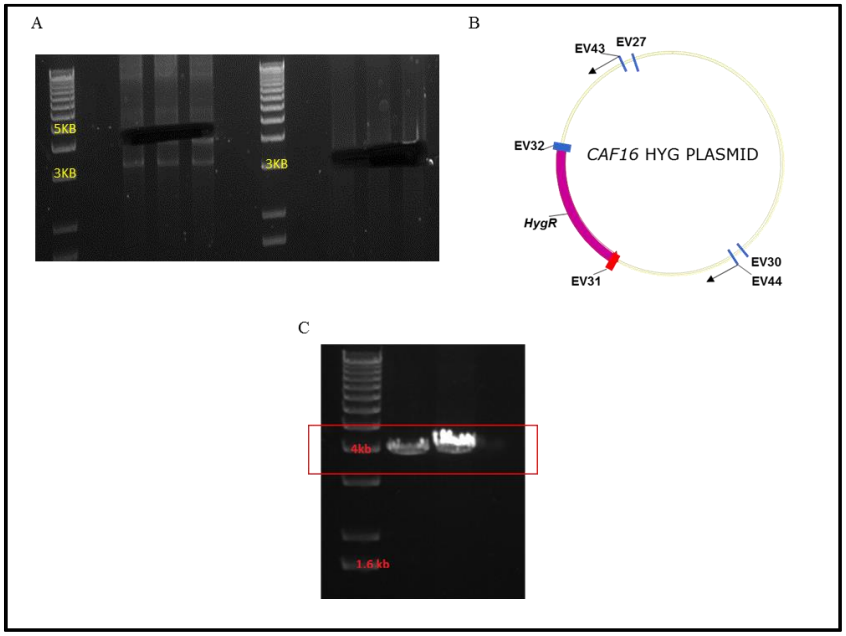

Figure 2.8 Development of △*caf16* Plasmid. A. Gel electrophoresis picture provides evidence of the restriction enzyme cut fragment from △*caf16* and pSM563 (pBluSKP) that were used for purification and ligation. △*caf16* was cut at 4.4kb and the plasmid was cut at 2.9kb. B. Graphical representation of the plasmid that was created after the fragments mentioned previously were ligated (Vector NTI Image). Illustration also shows the primer placement for the final fragment that was used for fungal transformation (EV43 & EV44). C. Gel electrophoresis image from the PCR product created using primers EV43 & EV44, product size 4kb.

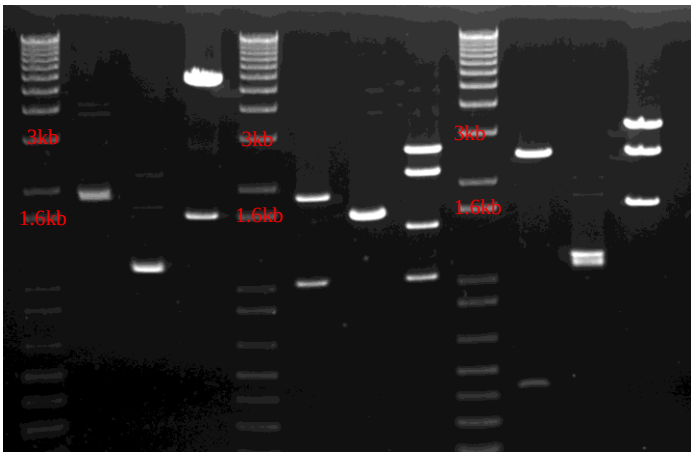

Figure 2.9 Diagnostic Restriction Enzyme Digest to Confirm Δ*caf16* plasmid fragment using *Pvu*I, *Pvu*II, and *Aat*II cutters. Lane 1, 5, and 9 were 1kb+ markers. Lanes 2-4:⧋*caf16* plasmid DNA cut with *Aat*II-Expected bands: 5708 bp, 1671bp, Lanes 6-8: ⧋*caf16* plasmid DNA cut with *Pvu*I-Expected band: 2653bp, 2194bp, 1487bp, 1045bp, Lanes 10-12: ⧋*caf16* plasmid DNA cut with *Pvu*II-Expected bands: 3191bp, 2513bp, 1675bp.

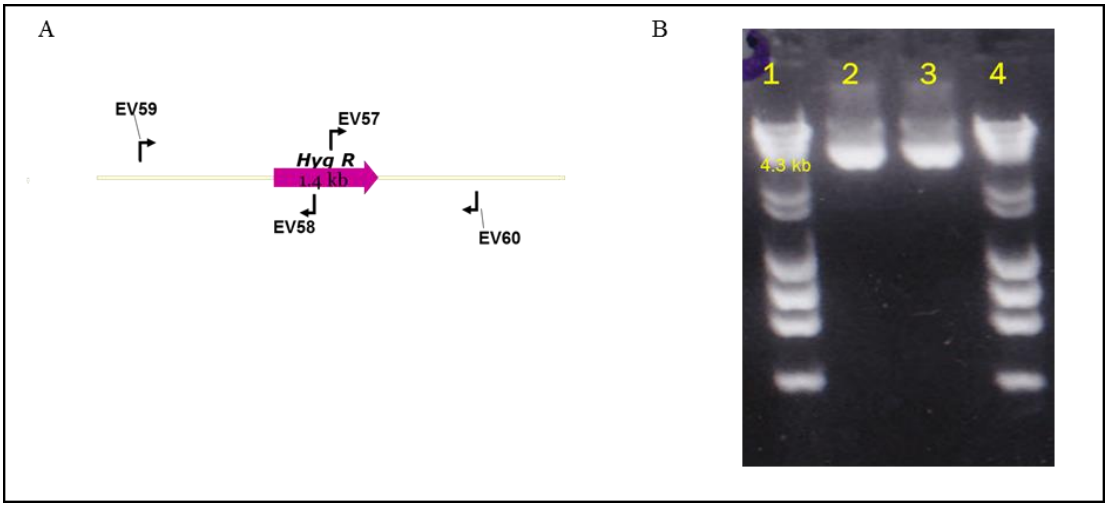

Figure 2.10 ⧋*caf16* Design and Primer Effectiveness Confirmatory PCR. A. Graphical representation (Vector NTI) showing primer placement for primers to use for transformation. B. Gel electrophoresis image using primers EV59 & EV60 to provide evidence that the outer primers worked. Lambda *Hind*III/*Hae*III Marker was used in lanes 1 & 4. 2 replicates shown in lanes 2 & 3 for primer EV59 & EV60, expected product size, 5kb.

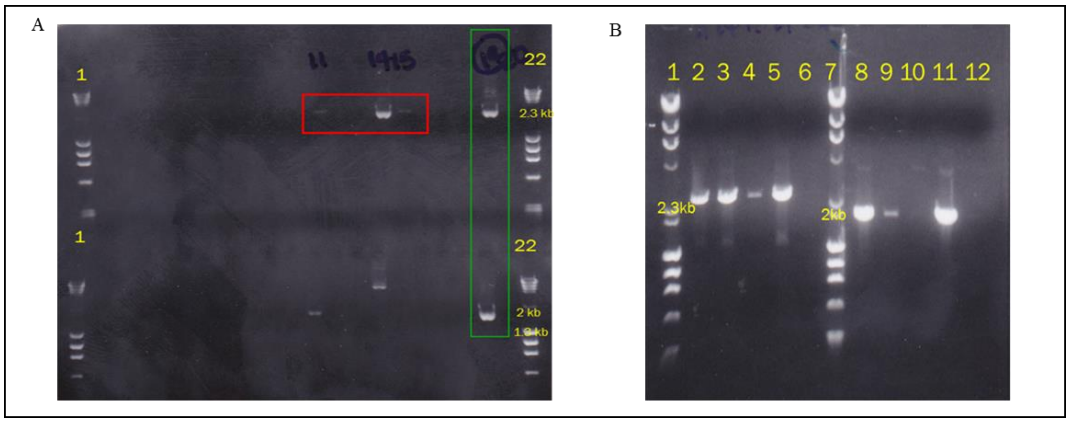

Figure 2.11 △*caf16* Confirmatory PCR Products from fungal mutant via Gel Electrophoresis. A. Lambda *Hind*II/*Hae*III Marker was used in lanes 1 & 22. 20 transformants were tested. Top of gel shows primer set EV59/EV58 and should generate a fragment 2.4kb in size. Bottom of gel shows primer set EV57/EV60 and should generate a fragment 1.8kb in size. B. Lane 1-Lambda *Hind*III/*Hae*III Marker, Lane 2-△*caf16* Transformant 11-5', Lane 3-△*caf16* Transformant 14-5', Lane 4-△*caf16* Transformant 15-5', Lane 5-△*caf16* Transformant 19-5', Lane 6-△*caf16* Transformant 20-5', Lane 7-Lambda *Hind*III/*Hae*III Marker, Lane 8-△*caf16* Transformant 11-3', Lane 9-△*caf16* Transformant 14-3', Lane 10-△*caf16* Transformant 15-3', Lane 11-△*caf16* Transformant 19-3', Lane 12-△*caf16* Transformant 20-3'.

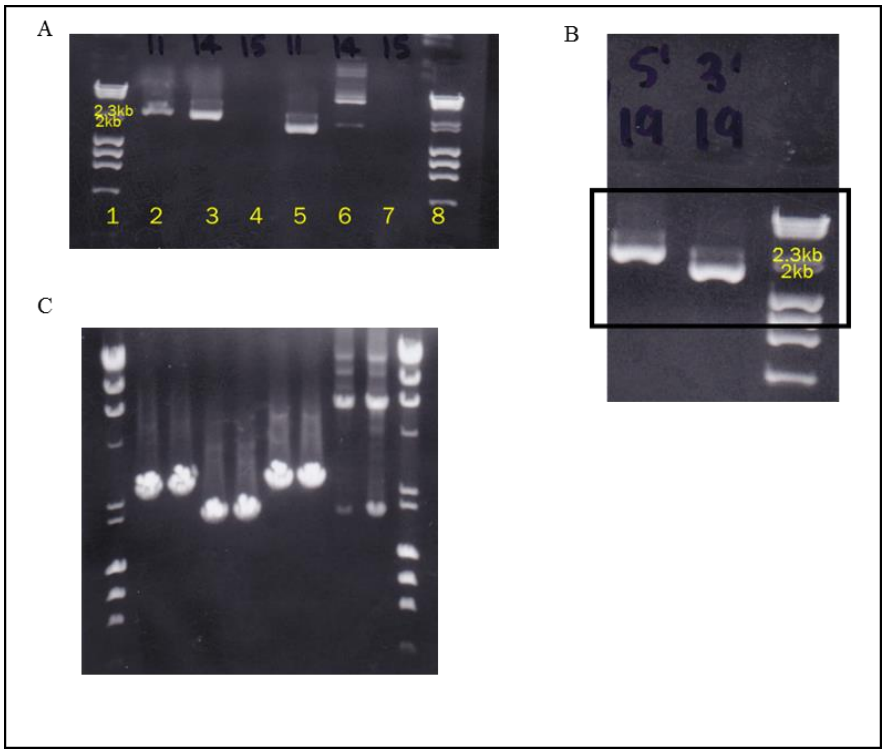

Figure 2.12 Confirmatory PCRs via Gel Electrophoresis. A. Lane 1-Lambda *Hind*III/*Hae*III Marker, Lane 2-△*caf16* Transformant 11-5', Lane 3-△*caf16* Transformant 14-5', Lane 4-△*caf16* Transformant 15-5', Lane 5-△*caf16* Transformant 11-3', Lane 6-△*caf16* Transformant 14-3', Lane 7-△*caf16* Transformant 15-3', Lane 8-Lambda *Hind*III/*Hae*III Marker. B. Gel electrophoresis image, Lane 1 △*caf16* Transformant 19-5', Lane 2 △*caf16* Transformant 19-3', Lane 3- Lambda *Hind*III/*Hae*III Marker. C. Lane 1-Lambda *Hind*III/*Hae*III Marker, Lane 2-△*caf16* Transformant 11-5', Lane 3-△*caf16* Transformant 11-5, Lane 4-△*caf16* Transformant 11-3', Lane 5-△*caf16* Transformant 11-3', Lane 6-△*caf16* Transformant 14-5', Lane 7-△*caf16* Transformant 14-5', Lane 8-△*caf16* Transformant 14-3', Lane 9-△*caf16* Transformant 14-3', Lane 10-Lambda *Hind*III/*Hae*III Marker.

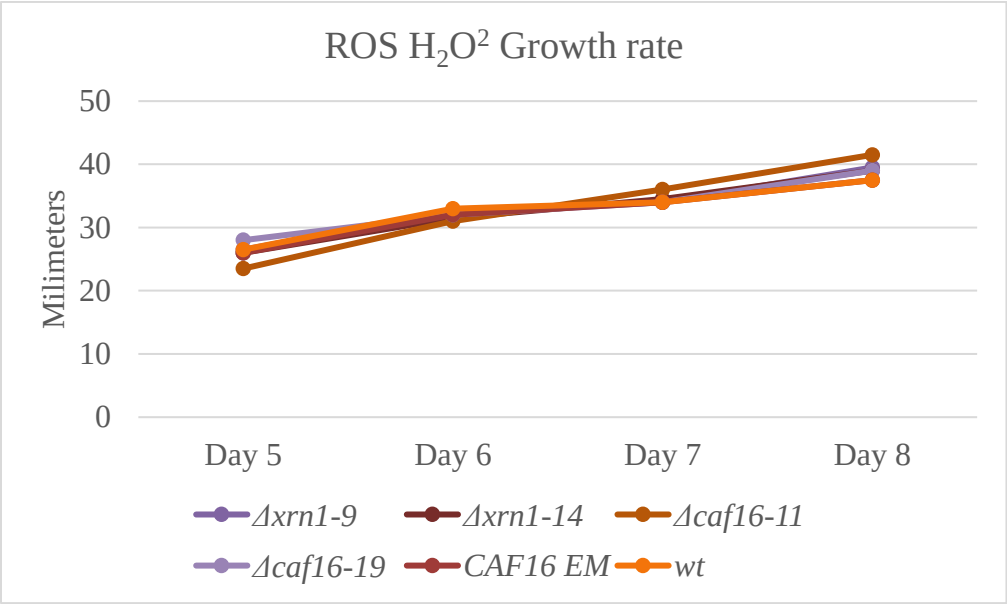

Figure 2.13 Growth rate analysis on ROS (H_2O_2) media, over 4 days, beginning on Day 5 post inoculation. Averages represented in this chart are from 3 technical replicates.

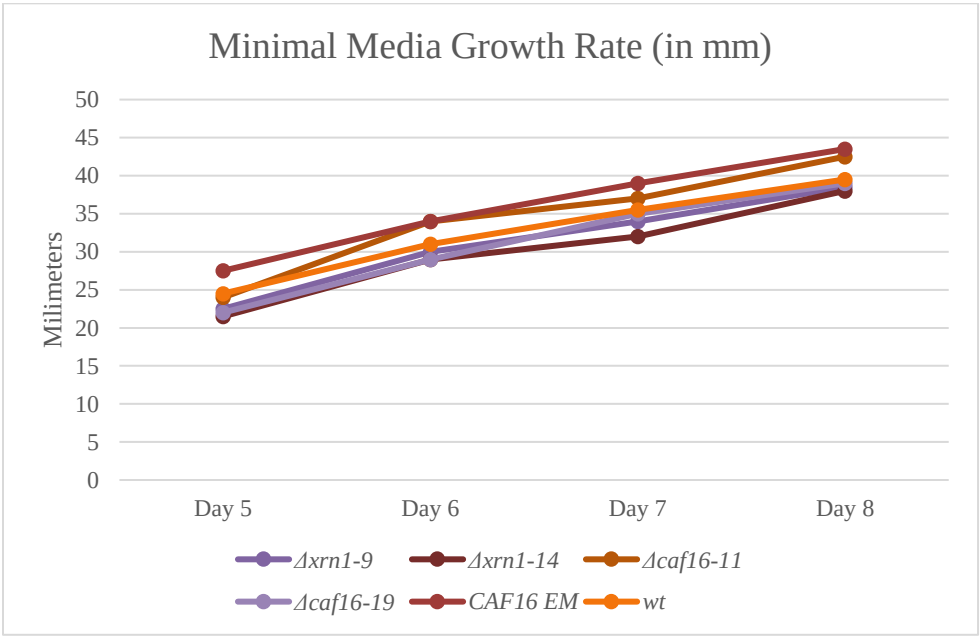

Figure 2.14 Growth rate analysis on minimal media, over 4 days, beginning on Day 5 post inoculation. Averages represented in this chart are from 3 technical replicates.

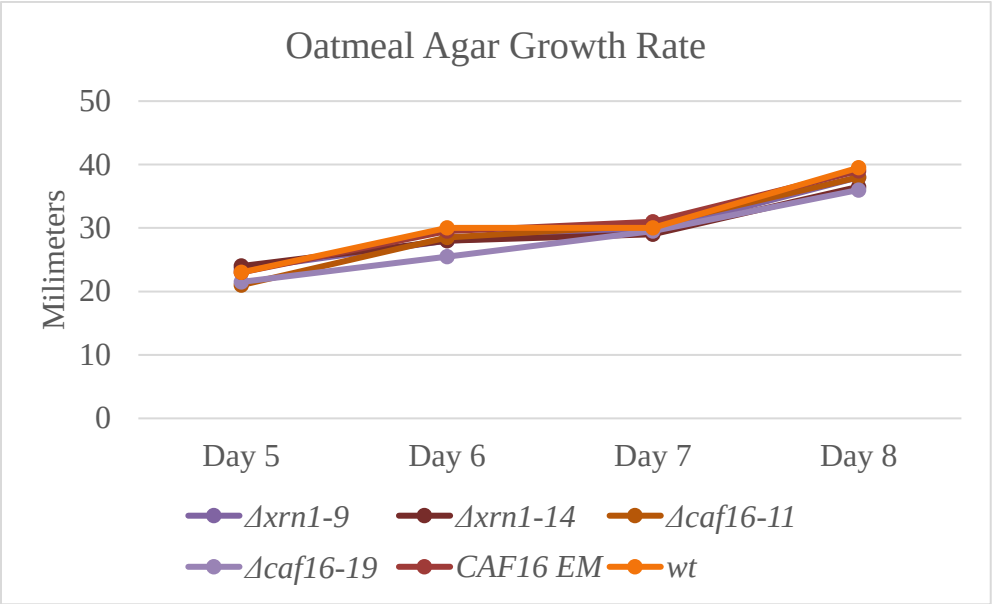

Figure 2.15 Growth rate analysis on oatmeal agar media, over 4 days, beginning on Day 5 post inoculation. Averages represented in this chart are from 3 technical replicates.

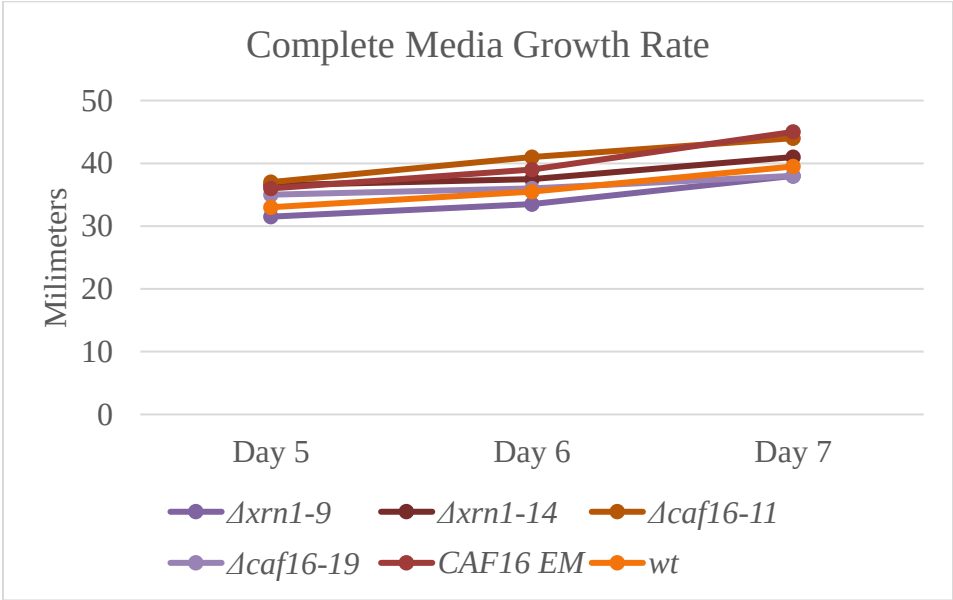

Figure 2.16 Growth rate analysis on complete media agar, over 4 days, beginning on Day 5 post inoculation. Averages represented in this chart are from 3 technical replicates.

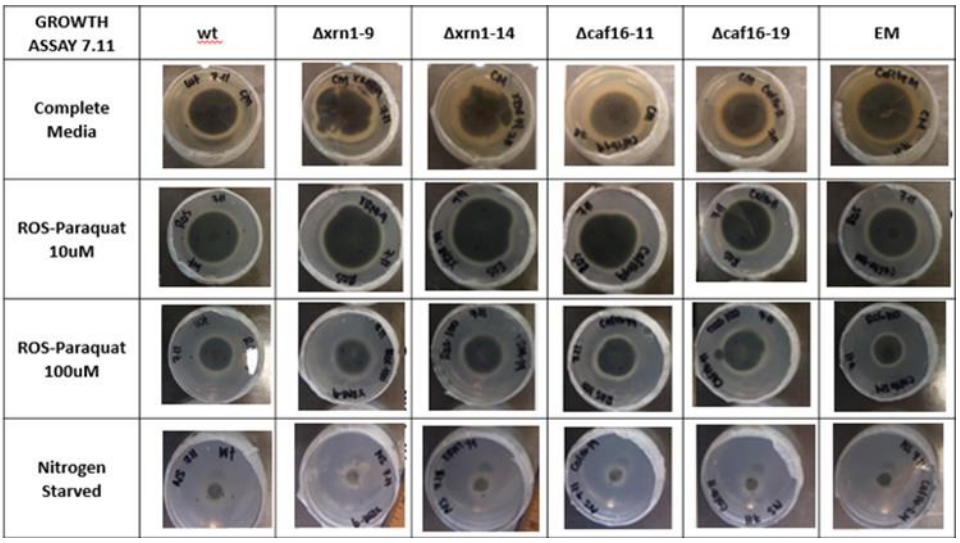

Figure 2.17 Images taken of plates during Growth Assay, Day 7 post inoculation. Wild-type 4091-5-8 is indicated by "wt" and *CAF16* ectopic mutant is indicated by "EM:

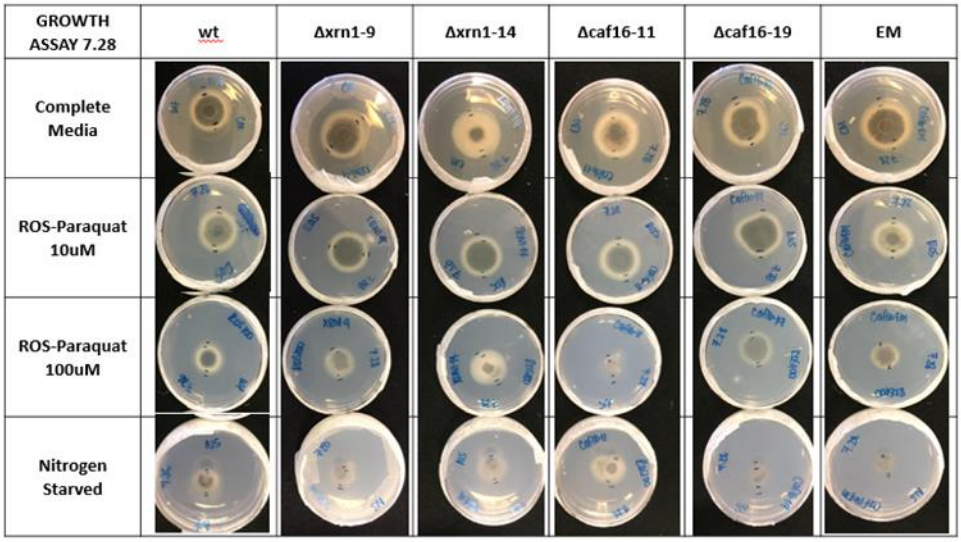

Figure 2.18 Images taken of plates during Growth Assay, 2nd Technical Replicate, Day 7 Post inoculation. Wild-type 4091-5-8 is indicated by "wt" and *CAF16* ectopic mutant is indicated by "EM:

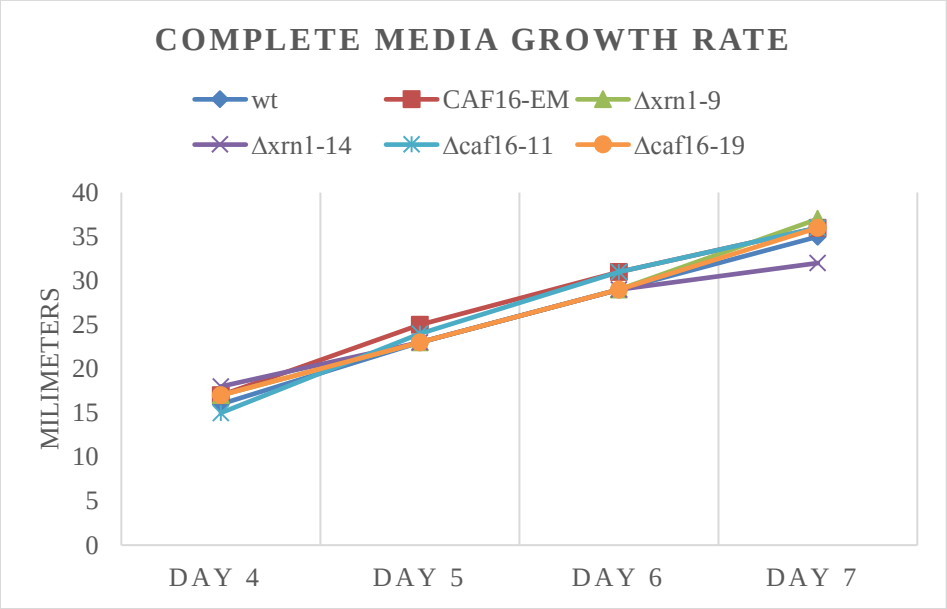

Figure 2.19 Growth analysis on complete media, 2nd biological replicate, over 4 days. Complete media serves as the control media in assays. Averages represented in this chart are from 2 technical replicates.

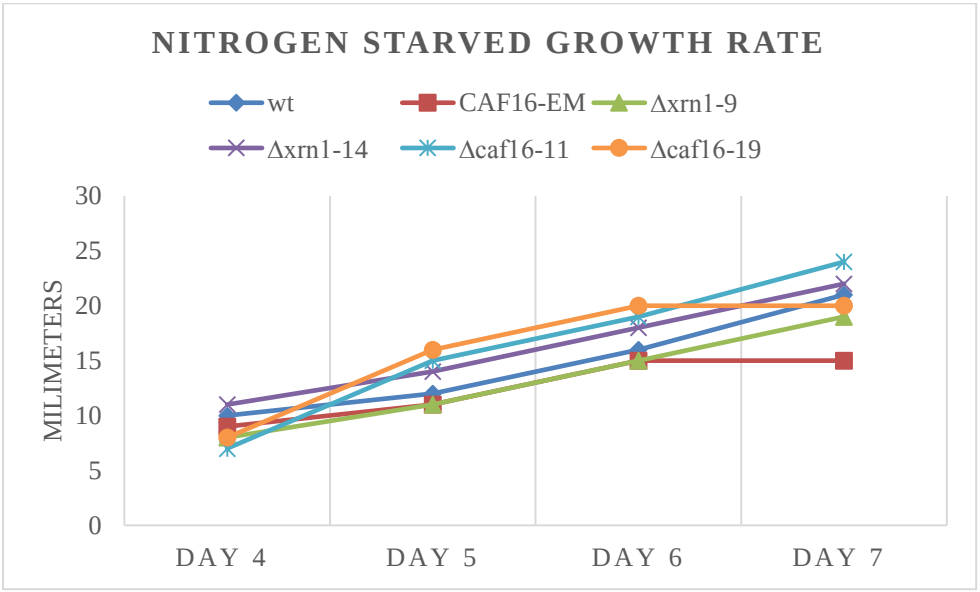

Figure 2.20 Growth analysis on nitrogen starved media, over 4 days. Measurements were taken on Day 5 post-inoculation. Averages represented in this chart are from 2 technical replicates.

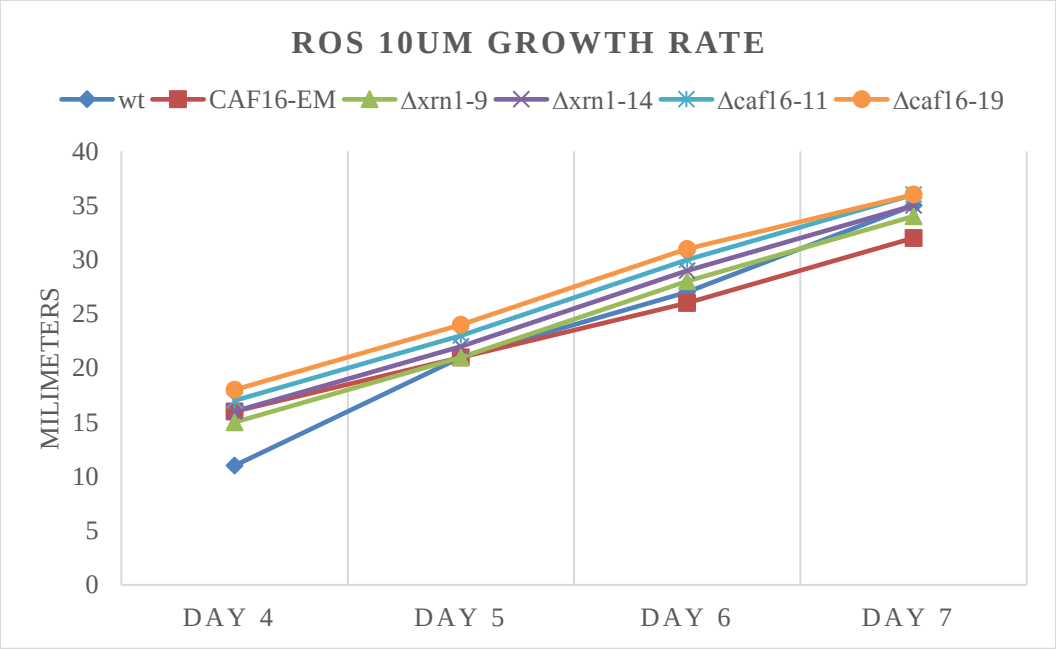

Figure 2.21 Growth analysis on ROS media using Paraquat at 10uM concentration, over 4 days. Measurements began on Day 5 post inoculation. Averages represented in this chart are from 2 technical replicates.

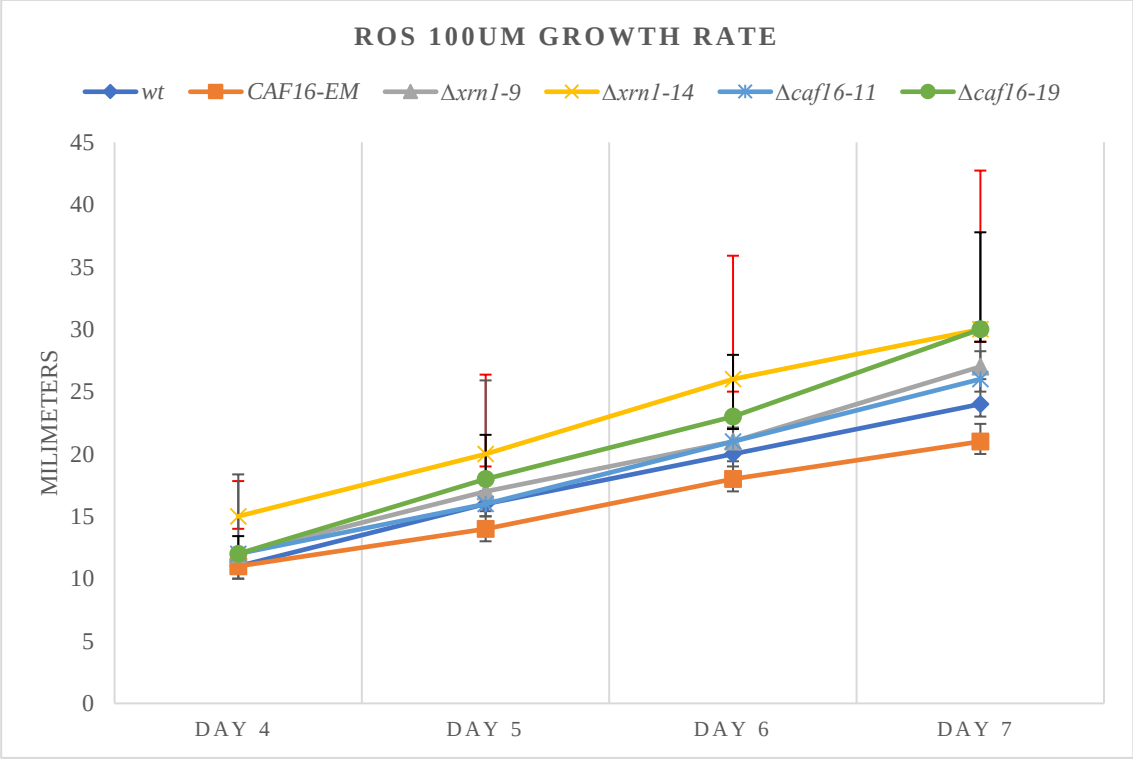

Figure 2.22 Growth analysis on ROS media using Paraquat at 100µM concentration, over 4 days. Measurements began on Day 5 post inoculation. Standard errors bars were based on two technical replicates.

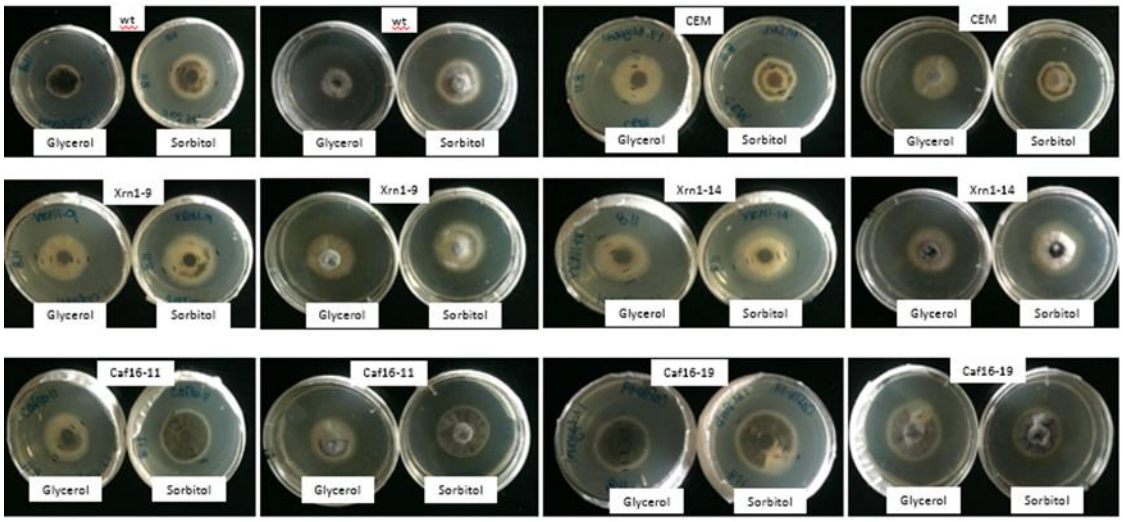

Figure 2.23 Images (top and bottom of plate) from the Glycerol (10%) and Sorbitol (1M) Hyperosmotic Stress Assay. Images taken Day 5 post-inoculation. Wild-type 4091-5-8 is indicated by "wt" and *CAF16* ectopic mutant is indicated by "EM:

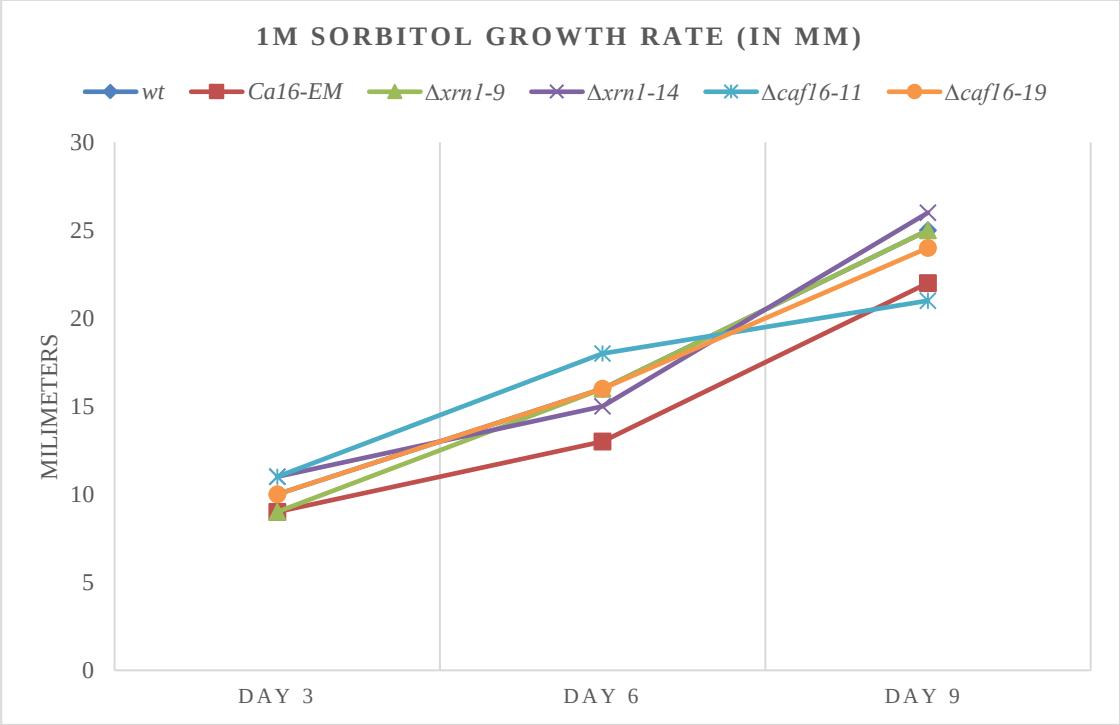

Figure 2.24 Growth analysis from 1M sorbitol assay, measure Day 3, 6, and 9. Measurements began on Day 3 post inoculation. Data is based off one technical replicate due to contamination in second set.

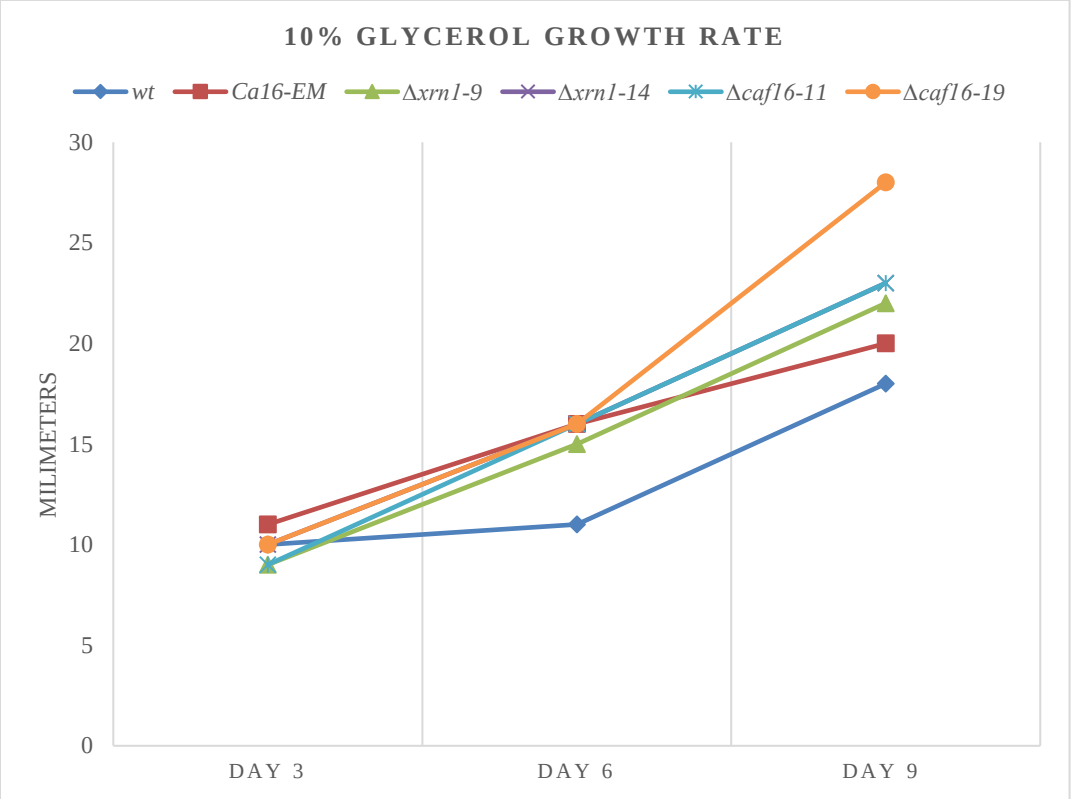

Figure 2.25 Growth analysis from 10% glycerol assay, measure Day 3, 6, and 9. Measurements began on Day 3 post inoculation. Data is based off one technical replicate due to contamination in second set.

Chapter 3

MOLECULAR PHENOTYPIC ANALYSIS BY qPCR

3.1 Methods

3.1.1 RNA Isolation and cDNA Synthesis

We isolated RNA from the mutants that were kept in the stress growth conditions. Much like the growth rate assay on agar, we used complete media (as the standard), minimal media, reactive oxygen species media, and 20% glycerol media. All recipes were performed in the same way as previously mentioned, with the removal of the agar component for liquid media. ROS media was prepared at a 10μM and 100μM concentration. Cultures were grown until Day 6 and were immediately flash-frozen in liquid nitrogen after vacuum filtering the liquid media from the culture on a sterile filter paper and vacuum Buchner funnel. The fungal mat was then pulverized into a fine powder and approximately 200μg were added to a sterile Eppendorf tube. One milliliter of TRIzol (Invitrogen) reagent was used for each reaction. The protocol for isolating RNA using TRIzol reagent was followed in its entirety. The isolated RNA was then used to make cDNA according to the QuantiTect Reverse Transcription Handbook protocol, revised 03/2009, page 12-13.

3.1.2 qRT-PCR Program Set Up

Quantitative real time reverse transcription PCR (real time qRT-PCR) was performed using primer pairs to test for reciprocal expression in the mutants. For △*caf16* mutants, we measured levels of *XRN1* transcripts to determine what occurs in the absence of the other gene. For △*xrn1*, we measured expression levels of *CAF16* transcripts. For internal control purposes, we used the housekeeping gene, ubiquitin

conjugating enzyme, *UBC*, and glyceraldehyde-3-phosphate dehydrogenase *GAPDH*. These are reference genes that are related to basic and structural cell processes [27]. Primers used in the assay are listed in Table 2.1. PCR reaction conditions were as follows for a 20µl reaction: 9µl H2O, 9µl 5 Prime SYBR Green Master Mix (Fisher Scientific), 0.5µl Forward Primer (Concentration:100nM; Integrated DNA Technologies), 0.5µl Reverse Primer (Concentration:100nM; Integrated DNA Technologies) and 1µl template DNA. Conditions for real-time quantitative RT-PCR conditions were as follows (40 cycles): 95°C for 2 min; 95°C for 15 sec, 55°C for 15 sec, 68°C for 20 sec; For melting curve: 95°C for 15 sec; 60°C for 15 sec, 95°C for 15 sec; lid temperature constant at 105°C. Primer pairs used for expression analysis by qPCR of *DCS1* were EV72 and EV73, EV74 and EV75, EV76 and EV77, and, EV78 and EV79. Primer pairs used for expression analysis by qPCR of *POR1* were EV80 and EV81, EV82 and EV83, EV84 and EV85, and, EV86 and EV87 (Table 2.1). The $2^{(-\Delta\Delta Ct)}$ method was used for analyzing the data. ΔΔCt is defined as ΔCt treatment - ΔΔCt calibrator. cDNA from the strain 4091-5-8 in complete media was used as the calibrator for comparison of gene expression in ROS (Paraquat), minimal, and 20% glycerol media growth conditions in the mutant △*caf16* and △*xrn1* lines, as well as the ectopic mutant, *CAF16*-EM and Wild-Type. For both the ΔCt treatment and ΔCt calibrator, ΔCt is defined as Ct gene - Ct housekeeping gene, *GAPDH*.

3.2 Results

3.2.1 RNA Isolation

To test our samples in a real-time quantitative PCR, RNA was extracted and isolated from all samples in various stress and non-stress media and then later made

into complement DNA. Nanodrop values for the RNA isolations from complete media, minimal media, and ROS (10μM) are available in Tables A1.1, A1.2, A1.3, A1.4, and A1.5. Two biological replicates were performed over two different dates as well as two technical replicates performed per sample. Samples shaded in gray in the Nanodrop value tables were used for cDNA synthesis.

3.2.2 qPCR Analysis

3.2.2.1 Growth conditions, Complete, ROS, and Minimal Media *XRN1*/*CAF16*

To test expression of *XRN1* and *CAF16* transcripts in the mutants, we conducted a series of qPCRs. Using a template designed to calculate the fold change expression between the mutants ($2^{-\Delta\Delta CT}$), values were normalized to the housekeeping genes, *UBC* and *GAPDH* separately, as well as to the calibrator, which was the wild type fungus growing in complete media. Figure 3.1 outlines the fold change differences between the mutants in response to their growth environment. We expect △*xrn1* mutants to be less than 1 as they do not contain the *XRN1* transcripts that the primers were designed to test. Mutant △*xrn1-9*, however had an increase in expression in Paraquat media. We see an increase in ROS and complete media growth conditions in one of the mutants, a decrease in ROS and complete media growth conditions in the other mutant, and substantial increase in minimal media growth conditions in both mutants. △*caf16* mutants show an increase of *XRN1* transcripts in minimal media and ROS media, and a decrease in expression in the complete media (calibrator). The ectopic mutant, *CAF16*-EM shows substantial increase in expression in the minimal media, no expression in complete media, and relative to wild-type for ROS media growth conditions. A student t-test was performed on this data and it was

revealed to not be statistically significant ($p > 0.05$). Figure 3.2 outlines fold change difference using *CAF16* primers. We expect to see no expression in the △*caf16* mutants, however we see increased expression in ROS and complete media growth conditions, and less expression to wild-type in minimal media growth conditions. The ectopic mutant show decreased levels of expression in ROS and complete media growth conditions, and a substantial increase in minimal media growth conditions. A student t-test was performed on this data and it was revealed to not be statistically significant ($p > 0.05$).

3.2.2.2 *DCS1*/*POR1* in Complete and Glycerol Media

To determine activity of *DCS1*, a scavenger decapping enzyme, and *POR1*, a mitochondrial porin, we conducted a series of qPCRs using primers designed within their sequences. Figure 3.3 shows substantial increase in expression of *DCS1* in mutants in complete media growth conditions, including the ectopic mutant. For glycerol media growth conditions, both △*xrn1* mutants, and △*caf16* mutants show a decrease to no expression of the transcript. As indicated by a student t-test, differences between glycerol and complete media were statistically significant ($p < 0.05$). Figure 3.4 outlines the analysis of *POR1* transcripts and shows an increase in expression in glycerol media for all mutants. In complete media growth conditions, there was an inconsistency in expression throughout the mutant lines. Based on a student t-test, difference between glycerol and completed media were statistically significant ($p<0.05$). Additional qPCRs are available in the Appendix, and are not statistically significant.

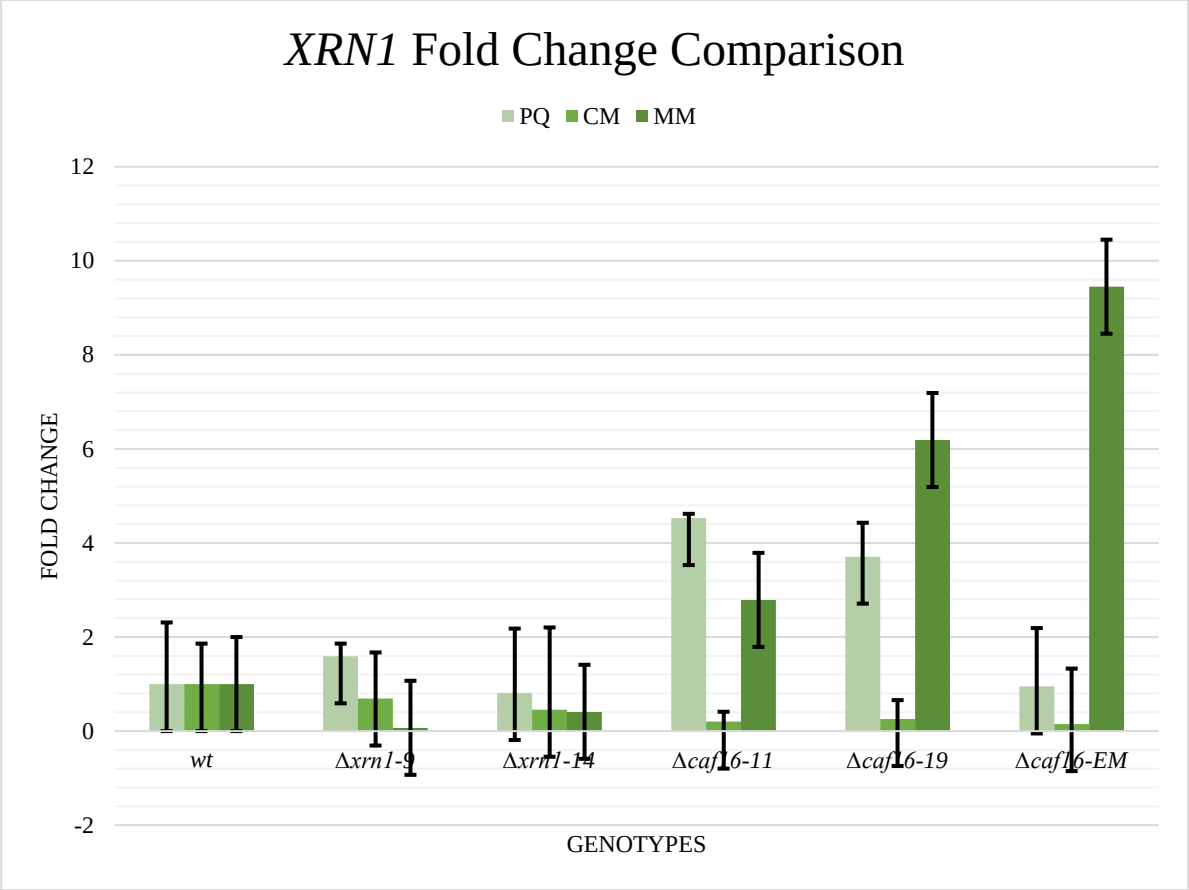

Figure 3.1 Fold Change Comparison for *XRN1* transcripts in mutants and wild-type in complete media (control), minimal media, and ROS media conditions. All values were normalized to the housekeeping gene *GAPDH* and to wild-type. Based on a student's T-test, this data has no statistical significance ($p>0.05$).

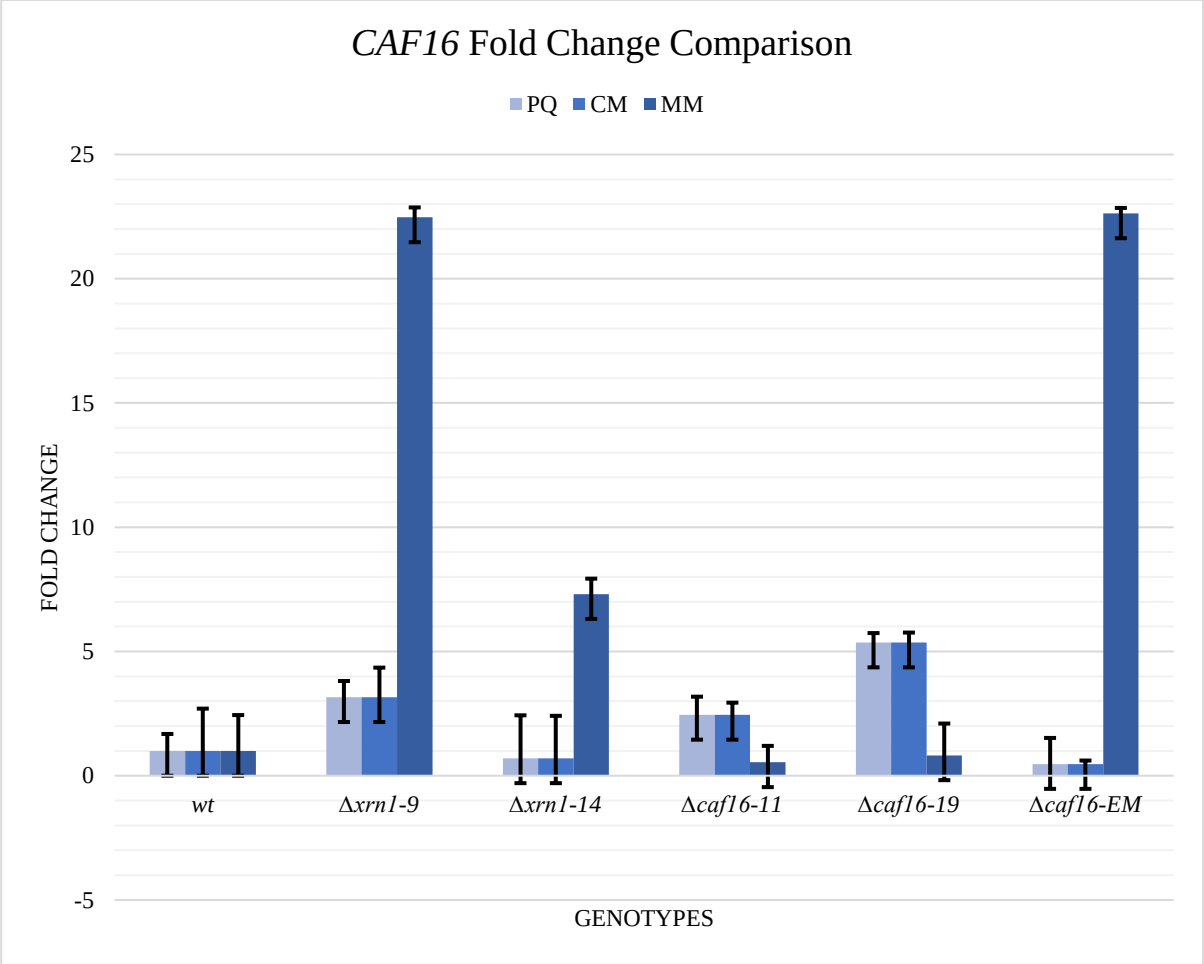

Figure 3.2 Fold Change Comparison for *CAF16* transcripts in mutants and wild-type in complete media (control), minimal media, and ROS media conditions. All values were normalized to the housekeeping gene *GAPDH* and to wild-type. Based on a student t-test, this data has no statistical significance ($p>0.05$).

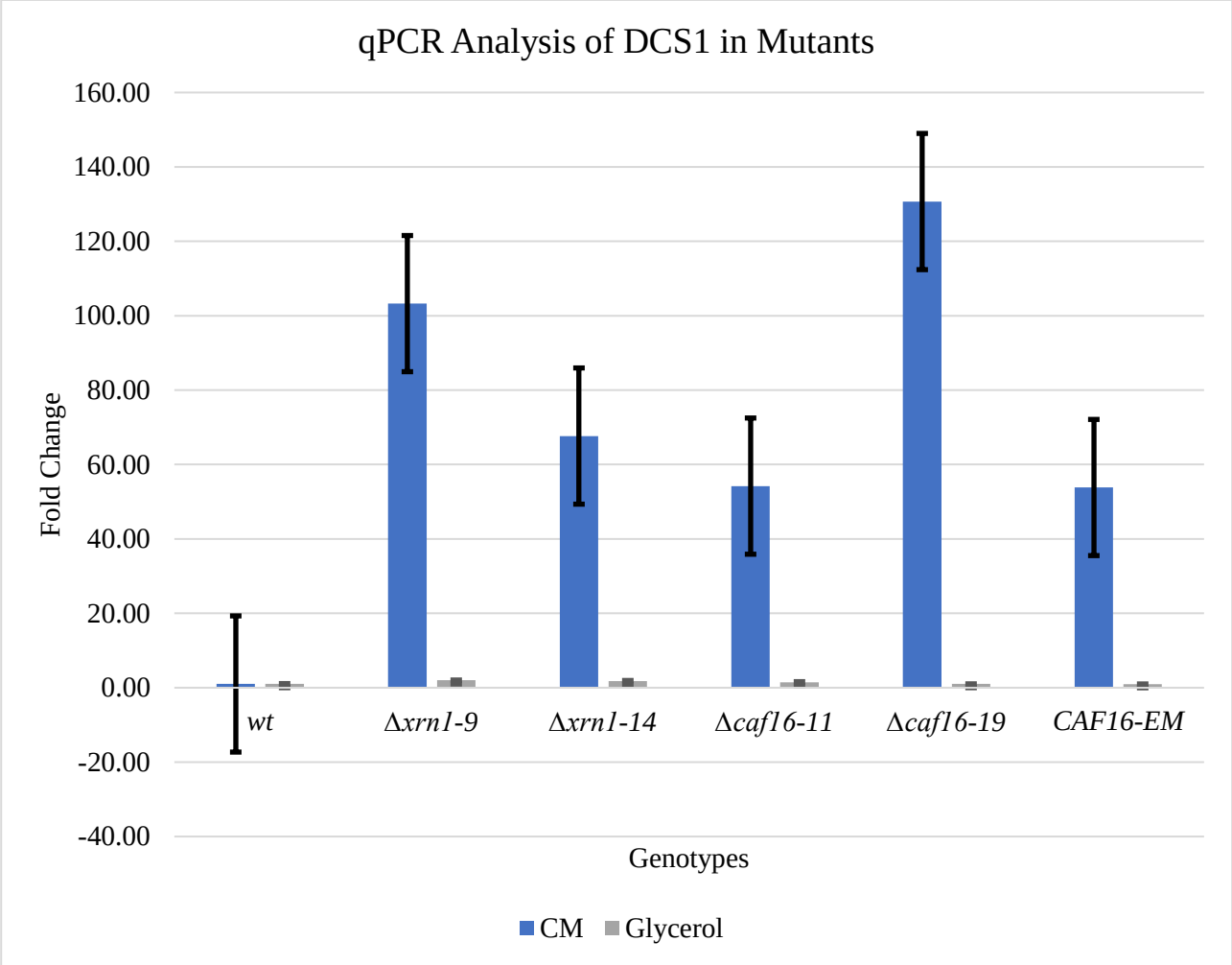

Figure 3.3 Fold change data from qPCR analysis of *DCS1* in mutants and wild-type in 20% glycerol media and complete media (control) conditions. Standard deviations were calculated based on two technical replicates. Primers EV 72 and EV73 were used for this qPCR data. Primers were designed around an intron to ensure mRNA transcripts. As indicated by a student t-test, differences between glycerol and complete media were statistically significant ($p < 0.05$).

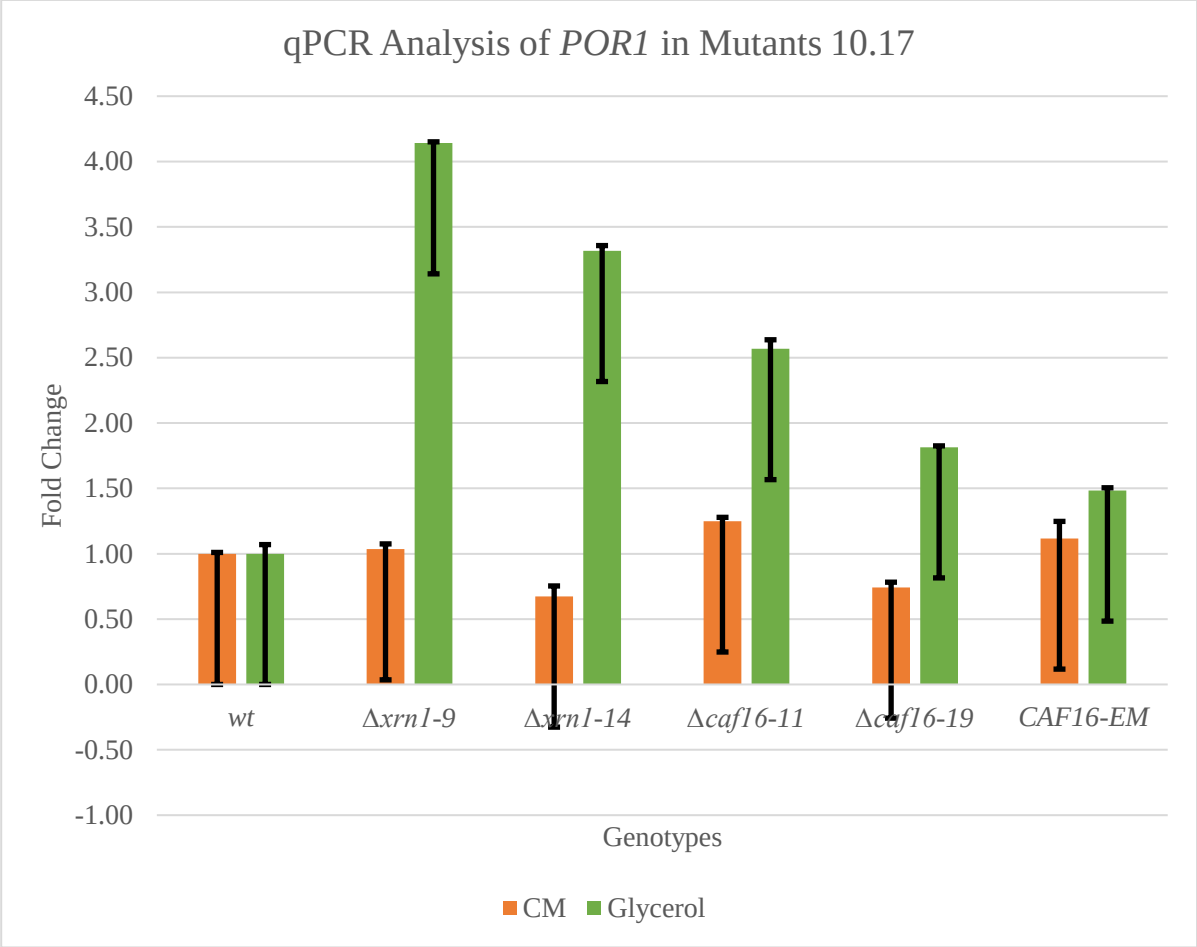

Figure 3.4 Fold change data from qPCR analysis of *POR1* in mutants and wild-type in 20% glycerol media and complete media (control) conditions. Standard deviations were calculated based on two technical replicates. Primers EV 80 and EV81 were used for this qPCR data. Primers were designed around an intron to ensure mRNA transcripts. As indicated by a student t-test, differences between glycerol and complete media were statistically significant ($p < 0.05$).

Chapter 4

PATHOGENESIS ASSAYS BY DETACHED LEAF AND WHOLE PLANT

4.1 Methods

4.1.1 Detached Leaf Assay

Wild-type strain, *M. oryzae* 4091-5-8, *⊿xrn1-9, ⊿xrn1-14, ⊿caf16-11, ⊿caf16-19, and CAF16*-EM (Ectopic Mutant) were grown on Malt Yeast Extract Agar (MYE) for a period of 10 days, which promotes production of asexual conidia for infection assays. Plates were kept in a climate controlled chamber set to 22°C and under fluorescent lights to increase sporulation. To collect spores, we used a 0.25% by volume gelatin solution (gelatin helps the spores stick to the plant leaves) and a sterile pipette tip to scrape the mycelia from the agar. Sterile cheesecloth was used to filter any debris from the gelatin-spore solution. Using a hemocytometer, cells were counted and all samples were diluted using the 0.25% gelatin solution to 1 x 10^5 spores per milliliter. The barely cultivar, Lacey (susceptible to *M. oryzae*), was grown in a growth chamber at 60% humidity, and 12-hour day/12-hour night cycles, at 24°C (day) and 22°C (night). For the assay, barley leaves were clipped at Day 8 and taped onto a water soaked paper towel in a 150mm x 15mm Petri plate to generate humidity. I used seven detached leaves from seven individual barley plants, for inoculation. Onto each leaf, three 20µl droplets were carefully pipetted onto the adaxial side. The 0.25% gelatin solution was used as the negative control in the assay. Closed Petri plates were placed under a storage bin for darkness for the first 24 hours to promote spore germination. To provide humidity, 4 beakers with boiling hot water were placed with the Petri plates under the storage bin. This was maintained for 24 hours to allow spore germination, appressorial development and penetration on the leaf. Once

completed, the residue from the solution was gently absorbed off the leaf using a Kimwipe. The Petri plates were put into a growth chamber under the same conditions as barley. On Day 5 post infection, the leaves were examined for lesion presence where the inoculum was placed and imaged.

4.1.2 Whole Plant Assay

Much like the detached leaf assay, wild-type, and mutants were prepared and spores were collected in the same manner. While generating the complement line, △*xrn1*-16 was discovered to be another *XRN1* knockout and contains a Bialophos integration This mutant was also used in this whole plant assay. Lacey barley was also grown in the same conditions as the detached leaf assay. Assays on whole plant were performed on 14-day old plants, which had a first true leaf about 4 inches long, and a second true leaf just emerging. I inoculated a total of six barley plants with each individual fungal line. For spore collection, 3 plates per sample were used to generate approximately 9 milliliters of spore-gelatin solution. For whole plant inoculation, an artist's airbrush was used to spray the spores evenly onto both sides of the barley leaf until the leaves were covered with tiny drops, but not before runoff occurred. The 0.25% gelatin solution was used as the negative control in the assay. The whole plants were placed into a storage bin for a 24-hour dark period. After the completion of the dark period, the infected whole plants were transferred to a transparent storage bin. Both storage bins were lined with a thick layer of wet paper towels and 4 beakers with hot water was placed in each corner of the storage bin to help maintain humidity. Bins were kept in the growth chambers at the settings that the uninfected barley was grown in. On Day 5 and 6 post infection, plants were observed for lesions. Data was collected

on the number of lesions present per leaf on Day 5. Images were taken on Day 5 and 6.

4.2 Results

4.2.1 Detached Leaf Assay

To determine phenotypical differences of disease in the △*caf16* and △*xrn1* mutants, we conducted a detached leaf assay. Lesions were observed on all leaves that were infected with spores. The control, 0.25% gelatin solution had no lesions. Lesions present on ⊿*xrn1-9* and ⊿*xrn1-14* had smaller to no lesions in comparison to Wild-type and ⊿*caf16* mutants. The ectopic mutant, *CAF16*-EM had lesions that were similar in size to Wild-type. Lesions from △*caf16* mutants had lesions that were also similar in size to the ectopic mutant and Wild-type. Measurements were not taken of lesions; Figures 4.1 and 4.2 provide visuals of this assay's results.

4.2.2 Whole Plant Assay

After phenotypical differences were notes in the △*xrn1* mutants, a whole plant assay was developed testing the △*xrn1* mutants, the complementation line, and wild-type. Mutants from △*caf16* were not used in the whole plant assay due to results from the detached leaf assay; lesions were similar in size to Wild-type. Two biological replicates were completed using two different storage bins for a set of 3 plants from each inoculum. One biological replicate, Trial 1, produced fewer lesions throughout the assay (Table 4.1). There were no lesions present on the control (0.25% gelatin solution) plants. In Trial 1, lesions from Wild-Type and the complement line, △*xrn1-C*, had three or fewer lesions. Lesion counts on the △*xrn1* mutants varied in Trial 1, with the more lesions present on △*xrn1-14* and △*xrn1-16* than △*xrn1-9*. Trial 2

produced more lesions overall in the plants (Table 4.1). Lesions were more prevalent and coalesced in Wild-Type, △*xrn1-C,* and △*xrn1-14.* Lesions present on △*xrn1-16* were also coalesced but fewer in number. Lesions present on △*xrn1-9* were smaller and fewer in number overall (Table 4.1). Images displayed in Figure 4.3-4.8 were taken on Day 5 (left) and Day 6 (right).

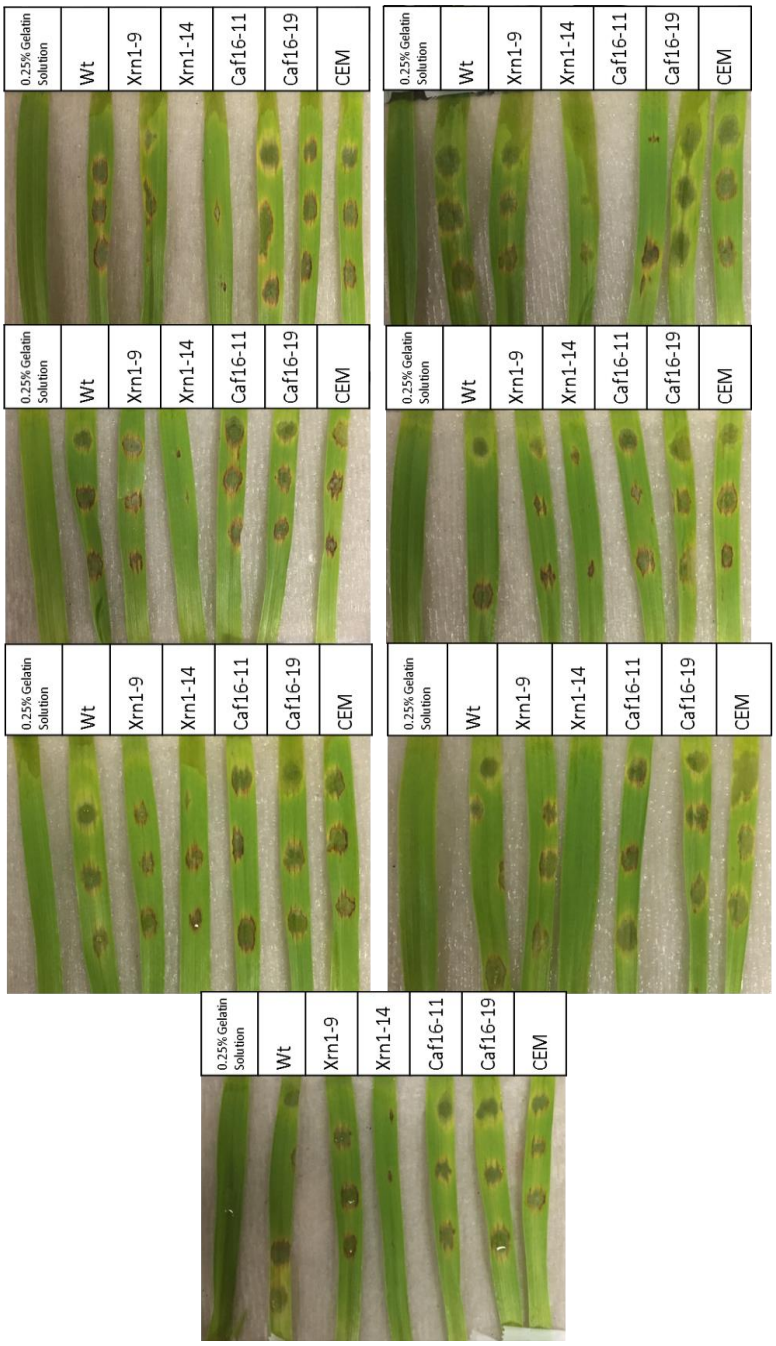

Figure 4.1 Images of Detached Leaf Assay (1st Set of Technical Replicates). Spores were collected from complete media plates and diluted to $1x10^5$ per milliliter using a 0.25% gelatin solution. Drop inoculation of 20µL were placed onto the adaxial side of the leaf. Left to right: Control-0.25% gelatin solution, wt-Wild-type 4091-5-8, ⧋*xrn1* mutants 9 and 14, ⧋*caf16* mutants 11 and 19, and CEM-Caf16 ectopic mutant.

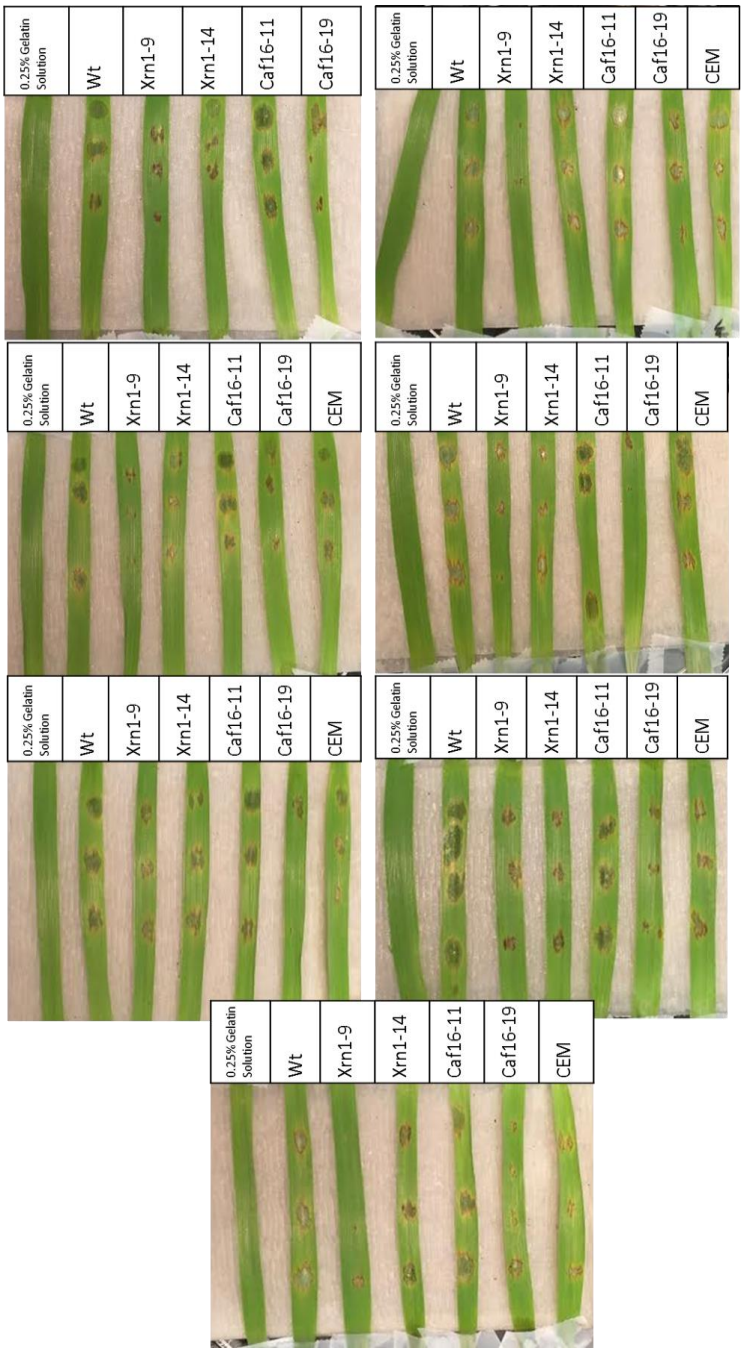

Figure 4.2 Images of Detached Leaf Assay (2nd Set of Technical Replicates. Spores were collected from complete media plates and diluted to 1x105 per milliliter using a 0.25% gelatin solution. Drop inoculation of 20µL were placed onto the adaxial side of the leaf. Left to right: Control-0.25% gelatin solution, wt-Wild-type 4091-5-8, △*xrn1* mutants 9 and 14, △*caf16* mutants 11 and 19, and CEM-Caf16 ectopic mutant.

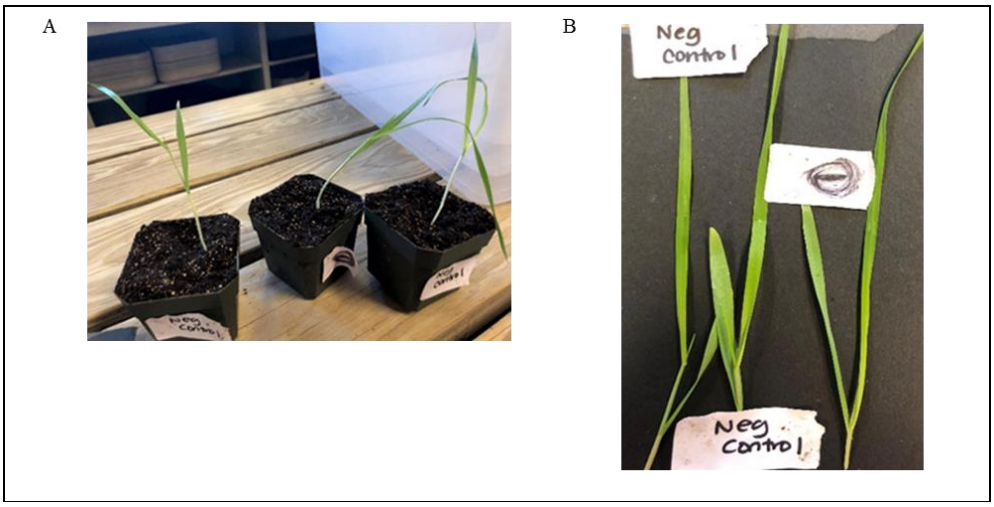

Figure 4.3 Whole plant inoculation Assay Image, Negative Control shown. A. Whole plant, image taken Day 5. B. Leaves were detached for image. Image taken Day 6.

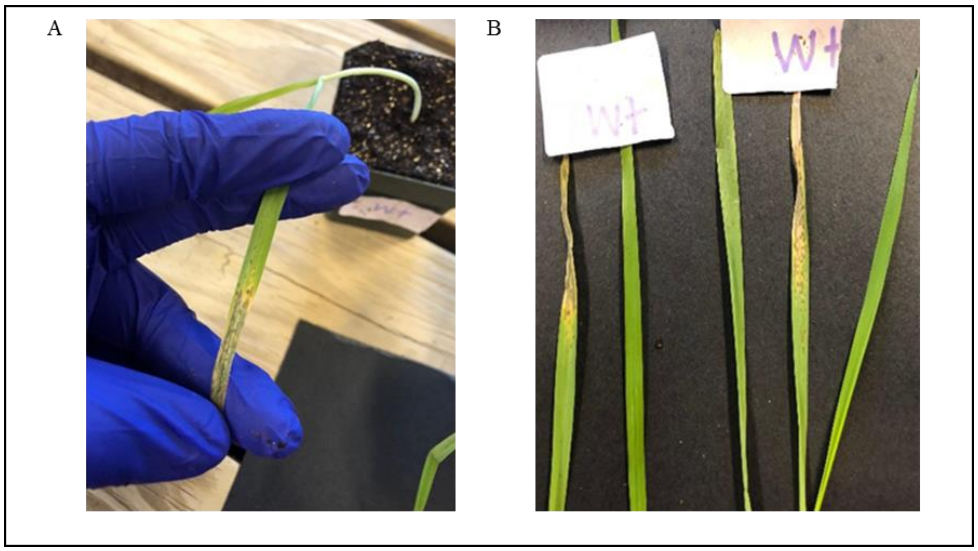

Figure 4.4 Whole plant inoculation Assay Image, Wild-type shown. Image taken Day 5. A. Whole plant, image taken Day 5. B. Leaves were detached for image. Image taken Day 6.

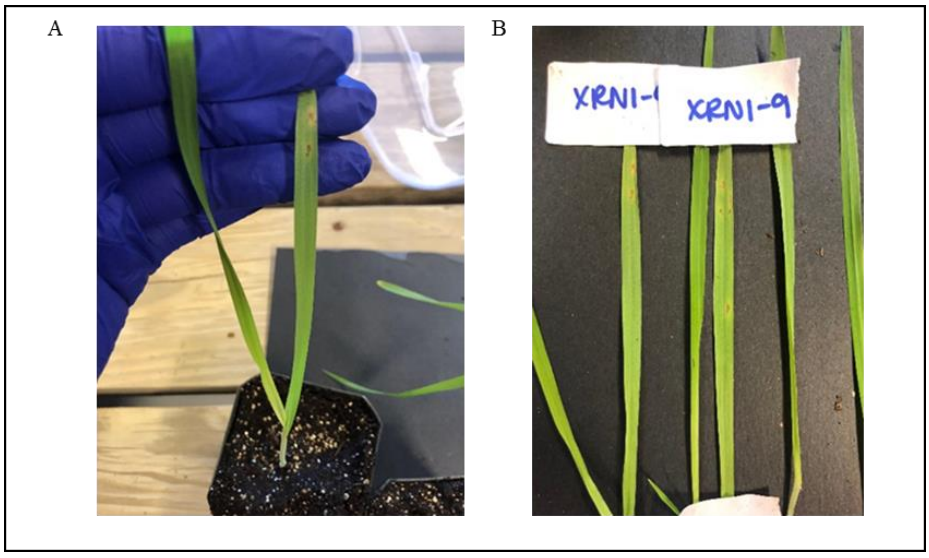

Figure 4.5 Whole plant inoculation Assay Image, *Δxrn1-9* shown. A. Whole plant, image taken Day 5. B. Leaves were detached for image. Image taken Day 6.

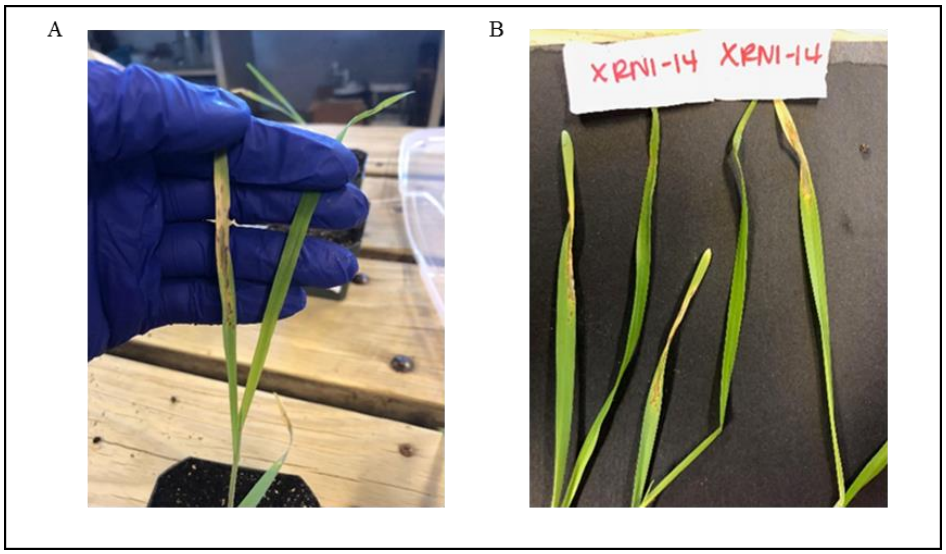

Figure 4.6 Whole plant inoculation Assay Image, *Δxrn1-14* shown. A. Whole plant, image taken Day 5. B. Leaves were detached for image. Image taken Day 6.

Figure 4.7 Whole plant inoculation Assay Image, *Δxrn1-16* shown. A. Whole plant, image taken Day 5. B. Leaves were detached for image. Image taken Day 6.

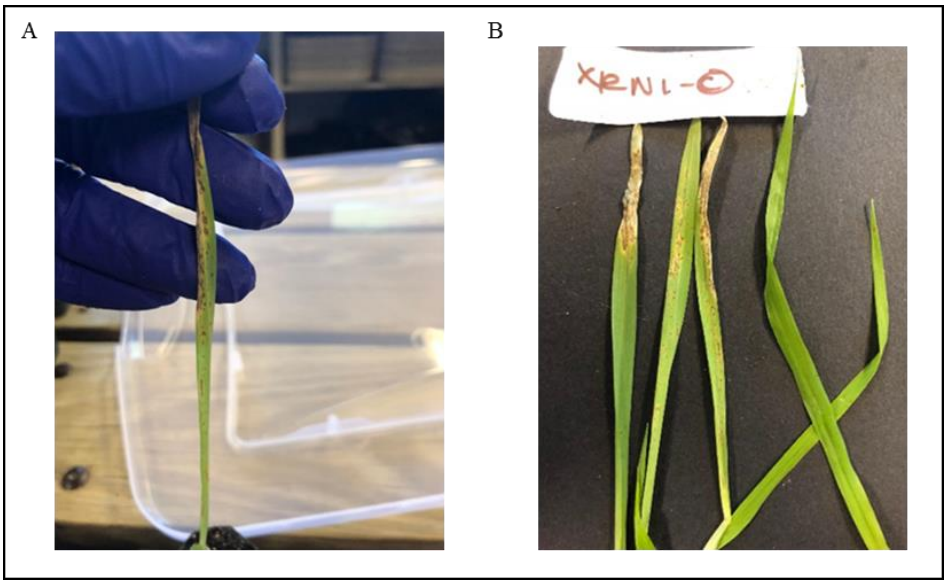

Figure 4.8 Whole plant inoculation Assay Image, *XRN1* (Complementation) shown. A. Whole plant, image taken Day 5. B. Leaves were detached for image. Image taken Day 6.

Table 4.1 Lesion Counts on Whole Plants in Path Assay

Plant #	**WT**		***Δxrn1-9***		***Δxrn1-14***		***Δxrn1-16***		***Δxrn1-C²***		**Gelatin**	
	Trial 1	Trial 2	Trial 1	Trial 2	Trial 1	Trial 2	Trial 1	Trial 2	Trial 1	Trial 2	Trial 1	Trial 2
1	2	10	8	20	2	TNTC	>25	0	3	>50	0	0
2	1	TNTC[1]	8	4	1	TNTC	1	32	3	TNTC	0	0
3	0	>50	1	3	TNTC	TNTC	6	>50	3	TNTC	0	0

[1] TNTC = too numerous to count
[2] complemented line
[3] Gelatin = negative control (no spores)

Chapter 5

DISCUSSION

5.1 Growth Rate Assay

In summary, mutants and wild-type behaved similarly in most stressful conditions (ROS (Paraquat and H_2O_2), nitrogen starved and minimal media). However, in the hyperosmotic assays, glycerol and sorbitol, there were some notable difference between the mutants and wild-type. In the 20% glycerol media, there was a slower growth of wild-type, with the ectopic mutant, *CAF16*-EM, behaving similarly to wild-type. As discussed in Sinturel et al, 2012, *XRN1* is necessary for growth in glycerol for yeast. However, this data suggests that in the absence of *XRN1*, there was more growth with $\triangle$*xrn1* than in wild-type. As this is contraindicative to what occurred in yeast, we suggest several additional time points as this assay had measurement every three days. Due to contamination, this data set was not reproduced in this research. In addition to increasing the number of time points, biological replicates along with statistical analyses (Student's T-test) to determine the validity of the data is recommended to determine persistence of $\triangle$*xrn1* mutants in glycerol media. The challenges faced in this assay were with the wild-type strain. Throughout our studies, we struggled to maintain a sporulating wild-type culture as it had begun to sector quickly in comparison to the mutants The mutants experienced much less sectoring and maintained higher conidia per milliliter when collected for pathogenesis assays on barley. We often started our wild-type from dried-down, frozen filter paper stocks but within the same cycle of plating, there was evidence of sectoring from the fungus, which is indicative of stress. The fungus grew as hyphae on the media plates, it just lacked significant numbers of spores. Since the wild-type experienced

symptoms of stress quicker than the mutants, it can be suggested that in the absence of *XRN1* or *CAF16,* the fungus continues to thrive in stressful conditions. To examine and determine if the mutants are maintaining better sporulation in stressful conditions, spores from the mutants and wild-type should be collected from complete media (as a control) and stress media conditions (i.e. ROS, minimal, nitrogen-starved, glycerol). Wild-type strain 4091-5-8 should be single spored and grown on complete media with filter papers for spore collection. Each assay should begin from filter paper stock to ensure a proper sporulation starting point.

5.2 qPCR Analysis

Results of the real-time quantitative RT-PCR (qRT-PCR) revealed the expected lower expression of *XRN1* transcripts in the *⊿xrn1* mutants. *Not*able differences in the *⊿caf16* mutants suggest an up-regulation of the *XRN1* transcripts in the absence of *CAF16* in stressful conditions, ROS and minimal media (Figure 3.1). However, the student t-test revealed that the values in this data set are statistically insignificant. This can be attributed to many errors in the process that is required to conduct a qPCR. The RNA isolation for some of the samples resulted in low 260/280 and 260/230 ratios indicating contaminants present in the sample. Also, since we experienced sectoring of wild-type on non-stress media throughout the assays, indicative that the organism is stressed, our values to which we normalized to may not be an accurate representation of expression in the organism. Our housekeeping gene, *UBC* also experienced difficulties in the qPCR as it had produced weak cycle thresholds. We used *GAPDH* to normalize our values to. Replication of this assay is required to further suggest an upregulation in the *CAF16* activity when *XRN1* is absent. The *CAF16* qPCRs reveal inconsistencies in the presence of *CAF16* transcripts

in the ⊿*caf16* mutants (Figure 3.2). There appears to be an upregulation in control media and ROS media conditions in both mutants with a lower expression in the minimal media conditions only. In looking at *CAF16* transcripts in ⊿*xrn1* mutants, a notable difference is in minimal media conditions, a stressor. However, because the data set was not statistically significant (student t-test), it is difficult to make suggestions of expression levels for *CAF16* and *XRN1* transcripts in the mutants.

5.2.1 qPCR analysis of *DCS1* and *POR1*

5.2.1.1 Analysis of *DCS1*

In Figure 3.3, the qRT-PCR analysis, in comparison to wild-type, we can see a substantial increase in expression of *DCS1* in all mutants in complete media growth conditions whereas in glycerol, the mutants had variable fold changes between 0.97 and 1.99. Though statistical analysis (student t-test) determined these values to be statistically significant, it is important to note the expression of wild-type in complete media over two technical replicates in the qPCR had a standard deviation of 8.17. Since values were normalized to wild-type as well as GAPDH, fold changes are much greater since the cycle threshold value of wild-type by technical replicate average was weaker. To correct this issue, it is recommended to run a qPCR in triplicate technical replicates with master mixes prepared to reduce pipetting error and validate data with standard deviations of 0.2 or less. As suggested in Sinturel et al, 2012, *DCS1*, the scavenger decapping enzyme, helps maintain activity of *XRN1* by decapping mRNA transcripts thus making it an ideal target for *XRN1*. We did see this in all mutants, however, due to the increase in expression in the ectopic mutant, this result requires further analysis of the ectopic mutant as the ectopic often behaved as a mutant in some

assays and as wild-type in others. It is critical to know the nature of where *HPH* integrated as it may be affecting the phenotypic analysis conducted within this research. The data set shown is from two technical replicates. This assay was repeated; however, the assay did not produce a cycle threshold value for wild-type and therefore, was not used. In glycerol growth media conditions, there were inconsistencies in expression between the *⊿caf16* mutants. *⊿caf16-19* behaved more like wild-type while *⊿caf16-11* increased in expression. Because *XRN1* is critical for growth on glycerol, in the absence of *XRN1* in glycerol conditions, the increase in expression in *DCS1* is not expected. However, since *DCS1* is a scavenger decapping enzyme, activity of *DCS1* could remain without *XRN1*, and there could be an accumulation of uncapped mRNAs which would lead to silencing of genes as suggested by Rymarquis et. al, 2011. To test this hypothesis, while incorporating the notion of the thriving fungal mutants, we could use RNA sequencing to determine the presence of viable full length mRNAs of virulence gene transcripts and compare them to Western blot analysis of their protein products. Since many genes have been characterized in *M. oryzae*, we can test a panel of stress response genes to determine if they have been silenced in *⊿xrn1* mutants. RNA sequencing would also provide a clearer indication of mRNA activity since qPCR does not provide information on the full-length mRNAs. Through RNA sequencing, we can also examine what occurs in the fungal mutants at various time points during the infection cycle. The observation that suggests that the mutants are thriving in stress conditions, we should expect to see an upregulation of virulence genes and down regulation of stress response genes. Mathioni et. al, 2011, conducted a study to test how fungi respond to biotic stress by analyzing the transcriptional profile of *M. oryzae*, when challenged with a bacterial

antagonist, *Lysobacter enzymogenes* [28]. This study saw an upregulation and down regulation of genes in the stress response category. Using the ⊿*caf16* and ⊿*xrn1* mutants, examination of stress response genes could assist in the hypothesis that the mutants respond to stress by continuing to thrive, with a significant down regulation of stress response genes. In Medina et. al, 2014, studies revealed that *XRN1* has a preferential activity to a subset of mRNAs; most affected were transcripts of highly transcribed genes [29]. Understanding the targets for *XRN1* in *M. oryzae* would allow us to understand the role it plays within mRNA degradation and gene regulation.

5.2.1.2 Analysis of *POR1*

In Figure 3.4, we analyzed transcripts of *POR1*, a mitochondrial porin needed for respiration. As suggested by Sinturel et al, 2012, in the absence *XRN1* in yeast, a decrease in expression in *POR1* is expected. In our assay, we see several inconsistencies in the organism's expression of *POR1*. In complete media growth conditions, we see slight increase in expression levels for △*xrn1-9*, and a slight decrease in expression for △*xrn1-14*. For △*caf16-11*, there is an increase in expression, while △*caf16-19* has a decrease in expression. As expected, the ectopic mutant behaved like wild-type in complete media growth conditions. For glycerol growth conditions, there is a substantial increase in expression in both △*xrn1* mutants as well as △*caf16* mutants. The ectopic mutant, also had an increase in expression for *POR1*. A student t-test determined these values to be statistically significant. However, the variance between mutants of the same knockout suggests error in the qPCR or variance in the integration of the knockout fragment. The challenges with qPCR were as expected with inconsistencies in cycle threshold (ct) values that were used to determine fold change. Also, the assays were normalized to two housekeeping

genes, *UBC* and *GAPDH*, which had some inconsistencies as well. Data normalized to *UBC* was not used as cycle threshold values were too weak. To determine a stronger correlation, we suggest additional technical replicates for this data set with master mixes generated to reduce well-to-well pipetting error.

5.3 Detached Leaf and Whole Plant Path Assay

In the detached leaf assay, the first set of technical replicates displayed visible smaller lesion sizes in the △*xrn1*-14 leaf (Figure 4.1). Though this assay also experienced similar difficulties with maintaining sporulation in the wild-type, we still were able to infect all leaves with a $1x10^5$ spores per milliliter. When the assay was repeated for the second set of technical replicates on a different date, we saw this similar phenotype with △*xrn1*-9 also displaying smaller lesions (Figure 4.2). This phenotype prompted us to repeat this assay on a whole plant. In whole plant assay, the spores were sprayed on to mimic environmental infection of the conidia spreading through the air. We saw unique phenotypes displayed by the △*xrn1* mutants. We also introduced mutant △*xrn1*-16 as this was discovered during the complementation assays. Overall, △*xrn1*-9 and △*xrn1*-16 displayed fewer lesions than wild-type and the complementation line. The complementation line behaved similar to wild-type in the amount of disease lesions produced. However, △*xrn1*-14 showed comparable disease lesions to wild-type suggesting inconsistencies in the genotypes. Although all mutants have been fully confirmed molecularly in the area the knockout was designed, we have no information at this point on the genomic sequence of the mutants. One possible hypothesis is that there could be multiple integration sites of the knockout fragment with *HPH* into the genome of the organism. Some challenges for this whole plant assay were in maintaining humidity in the chambers they were contained and

from chamber to chamber, there were differences in the number of lesions present throughout all the plants. This could be due to the amount of humidity that was contained in the chamber. Humidity is critical for sporulation and germination of the organism, therefore, to further analyze phenotypic differences, increasing the number of plants assayed is suggested.

5.4 Proposed Work

Throughout the phenotypic analysis of the mutants we generated in this research, it is important to note the importance of whole genome sequencing to understand what occurred as a result of the integration of the knockout fragment. Although the fragments were designed and tested to only insert via homologous recombination into one location, the number of insertions is unknown and may play a role in the differences we are seeing between mutants of the same genotype. We propose that the mutants in this study be fully sequenced. A Southern blot can also help determine the abundance of the insertion sequence, however, will not provide an exact number as whole genome sequencing would.

In our growth analysis assays, although we didn't see differences day to day, it is worth measuring on a smaller timescale to visualize subtle differences between the mutants to wild-type (e.g. every 6-8 hours). Since the data suggests overall persistence of the organism without *XRN1* or *CAF16*, the differences may be subtle as the organism adapts to its growing conditions. Since there were notable difference in the 20% glycerol media growth rates, we suggest increasing the concentration of glycerol to determine the response of the mutants and gathering data for a dose response curve for $\triangle$*xrn1* mutants. A spore count assay is recommended to determine if the mutants are thriving in stress conditions. Wild-type should be started from filter stock, grown

on a non-stress media and then inoculated on stress media. Each assay should begin from filter stock or single spored for wild-type since we do not want to measure wild-type as it begins to stress (sector) on non-stress media. This would eliminate variables in the spore counts when comparing non-stress to stress media. Mutants should also be grown the same way and spores should be collected and counted. Since mutants are remaining stable, while wild-type is sectoring over time, it is suggested that without *XRN1* or *CAF16*, the organism responds to stress by continuing to thrive in stressful conditions. As this then questions the need for *XRN1* or *CAF16*, however, the stress response can be interpreted as a mechanism of protection by the organism from a potential toxic stress. Without *XRN1* or *CAF16*, the organism is potentially subjecting itself to thrive with no regard to self-destruction. We suggest further examination of the mutants by analyzing virulence gene activity as previously mentioned in Section 5.2.1.1 Analysis of *DCS1*.

The phenotypic differences noted in the pathogenesis assays, both detached leaf and whole plant, suggested a decrease in virulence from the organism in the absence of *XRN1*. However, this decrease is inconsistent between the mutants from △*xrn1*. This further supports the need for the whole genome sequence to understand how the knockout occurred in the organism. As *XRN1* is a component in mRNA degradation, and mRNA degradation is a factor in gene regulation, we need to determine the true ⧋*xrn1* mutant phenotype of less or more lesions from the pathogenesis assays. The in vitro stress response, however, could be unrelated to the virulence pattern that we saw in plant pathogenesis assays. We propose an in-plant *M. oryzae* infection RNA extraction as presented in Sun et. al, 2015 and then conducting a qPCR analysis on a series of known virulence genes and stress response genes [30].

This would help us determine an upregulation or downregulation of virulence genes and stress response genes to compare to our in vitro studies. This would help us understand and generate conclusions on the role *XRN1* plays in mRNA degradation in *M. oryzae* and how mRNA degradation regulates virulence in the organism.

Most importantly, the phenotypic differences that were noted in the detached assay and whole plant tell us that *XRN1* is directly related to virulence. In order to ascertain this, both △*xrn1* and △*xrn1*-14 need to be fully characterized. Measuring the lesions from the detached leaf as well as the whole plant assay could provide additional data to support the effect *XRN1* has on virulence. When imaging, we suggest using scale bars and a color block (yellow to green) to provide a reference tool when analyzing the images of the mutants.

Continuing this research into components of mRNA degradation allows us to gain a deeper understanding of how gene regulation occurs in the organism. As this organism is of great agronomic importance, it's fully sequenced genome allows us to further our studies into the global mechanism by which *M. oryzae* regulates its genes, specifically virulence genes. Characterization of *XRN1* would enable to understand how this exoribonuclease destroys targeted mRNA transcripts and thereby regulating which gene are expressed in the organism. Through previous research in yeast and fungal relatives, and this current research, we have developed a framework into molecular plant-pathogen interactions.

REFERENCES

1. Wilson, R., & Talbot, N. (2009). Under pressure: Investigating the biology of plant infection by *Magnaporthe oryzae*. *Nature Reviews, 7,* 185-195

2. Geoghegan, Ivey. Investigating the Role of Chitin Deacetylation in *Magnaporthe oryzae*. Linacre College, University of Oxford, Oct. 2015.

3. Abdullah, A., Kobayashi, H., Matsumara, I., & Ito, S. (2015). World Rice Demands Towards 2050: Impact of Decreasing Demand of Per Capita Rice Consumption for China and India. *Research Gate,*1-18.

4. Dean, R. A., Talbot, N. J., Ebbole, D. J., Farman, M. L., Mitchell, T. K., Orbach, M. J., . . . Birren, B. W. (2005). The genome sequence of the rice blast fungus Magnaporthe grisea. *Nature,434,* 980-986.

5. Gowda, M., Shirke, M. D., Mahesh, H. B., Chandarana, P., Rajamani, A., & Chattoo, B. (2015). Genome analysis of rice-blast fungus *Magnaporthe oryzae* field isolates from southern India. *Genomics Data,5,* 284-291.

6. Talbot, N. J. (1995). Having a blast: Exploring pathogenicity of *Magnaporthe oryzae*. *Trends in Microbiology,3*(1), 9-16.

7. Balhadere, P. V. (1999). Identification of Pathogenicity Mutants of the Rice Blast Fungus Magnaporthe grisea by Insertional Mutagenesis. *MPMI,12*(2), 129-142.

8. Hamer, J. E., Howard, R. J., Chumley, F. G., Valent, B., et al. (1988). A mechanism for surface attachment in spores of a plant pathogenic fungus. *Science, 239,* 288-290.

9. Couch, B. C., Fudal, I., Lebrun, M., Tharreau, D., Valent, B., Van Kim, P., . . . Kohn, L. M. (2005). Origins of Host-Specific Populations of the Blast Pathogen *Magnaporthe oryzae* in Crop Domestication with Subsequent Expansion of Pandemic Clones on Rice and Weeds of Rice. *Genetics,170,* 613-630.

10. Jarosch, B., Collins, N. C., Zellerhoff, N., & Schaffrath, U. (2005). RAR1, ROR1, and the Actin Cytoskeleton Contribute to Basal Resistance to Magnaporthe grisea in Barley. *MPMI,18*(5), 397-404.

11. Verstegen, H., Koneke, O., Korzun, V., & Van Broock, R. (2014). The World Importance of Barley and Challenges to Further Improvements. *Biotechnological Approaches to Barley Improvement,69*, 3-19.

12. Kohli, M. M., Mehta, Y. R., Guzman, E., De Viedma, L., & Cubilla, L. E. (2011). Pyricularia Blast – a Threat to Wheat Cultivation. *Czech J. Genetics Plant Breed,47*, S130-S134.

13. Zhang, S. and Xu, J.-R. (2014). Effectors and effector delivery in *Magnaporthe oryzae*. *PLoS Pathogens*, *10*(1), 1-4.

14. Rymarquis, L. A., Souret, F. F., & Green, P. J. (2011). Evidence that XRN4, an *Arabidopsis* homolog of exoribonuclease *XRN1*, preferentially impacts transcripts with certain sequences or in particular functional categories. *RNA, 17*, 501-511.

15. Chen, C. A., & Shyu, A. (2011). Mechanisms of deadenylation-dependent decay. *Wiley Interdiscp Rev RNA,2*(2), 167-183.

16. Larimer, F. W., Hsu, C. L., Maupin, M. K., & Stevens, A. (1992). Characterization of the *XRN1* gene encoding a 5'-3' exoribonuclease: Sequence data and analysis of disparate protein and mRNA levels of gene-disrupted yeast cells. *Gene, 120*, 51-57.

17. Nagarajan, V. K., Jones, C. I., Newbury, S. F., & Green, P. J. (2013). XRN 5'-3' exoribonucleases: Structure, mechanisms, and functions. *Biochimica Et Biophysica Acta,1829*, 590-603.

18. Larimer, F. W., & Stevens, A. (1990). Disruption of the gene *XRN1*, coding for a 5'-3' exoribonuclease, restricts yeast cell growth. *Gene, 95*, 85-90.

19. Gazzani, S., Lawrenson, T., Woodward, C., Headon, D., & Sablowski, R. (2004). A Link Between mRNA Turnover and RNA Interference in Arabidopsis. *Science,306*, 1046-1048.

20. Sinturel, F., Brechemier-Baey, D., Kiledjian, M., Condon, C., & Benard, L. (2012). Activation of 5'-3' exoribonuclease Xrn1 by cofactor Dcs1 is essential for mitochondrial function in yeast. *Proceedings of the National Academy of Sciences,109*(21), 8264-8269.

21. Liu, H., Chiang, Y., Pan, J., Salvadore, C., Audino, D., Badarinarayana, V., . . . Denis, C. (2001). Characterization of CAF4 and *CAF16* Reveals a Functional Connection between the CCR4-NOT Complex and a Subset of SRB Proteins of the RNA Polymerase II Holoenzyme. *Journal of Biological Chemistry, 276(10),* 7541-7548.

22. Denis, C. L., Chiang, Y., Cui, Y., & Chen, J. (2001). Genetic Evidence Supports a Role for the Yeast CCR4-NOT Complex in Transcriptional Elongation. *Genetics,158*, 627-634.

23. Collart, M. A., & Panasenko, O. O. (2011). The CCR4-NOT Complex. *Gene,492*, 42-53. doi:10.1016

24. Pickart, C. M. (2001). Mechanisms Underlying Ubiquitination. *Annual Reviews: Biochemistry,70*, 503-533.

25. Funakoshi, Y., Doi, Y., Hosoda, N., Uchida, N., Osawa, M., Shimada, I., . . . Hoshino, S. (2007). Mechanism of mRNA deadenylation: Evidence for a molecular interplay between translation termination factor eRF3 and mRNA deadenylases. *Genes & Development,21*, 3135-3148.

26. Parsons, K. A., Chumley, F. G., & Valent, B. (1987). Genetic transformation of the fungal pathogen responsible for rice blast disease. *Proceedings of the National Academy of Sciences,84*, 4161-4165.

27. Huang, K., Czymmek, K. J., Caplan, J. L., Sweigard, J. A., & Donofrio, N. M. (2011). HYR1-Mediated Detoxification of Reactive Oxygen Species Is Required for Full Virulence in the Rice Blast Fungus. *PLoS Pathogens,7*(4), 1-18.

28. Mathioni, S. M., Belo, A., Rizzo, C. J., Dean, R. A., & Donofrio, N. M. (2011). Transcriptome profiling of the rice blast fungus during invasive plant infection and in vitro stresses. *BMC Genomic, 12*(49), 1-20.

29. Medina, D. A., Jordan-Pla, A., Millian-Zambrano, G., Chavez, S., Choder, M., & Perez-Ortin, J. E. (2014). Cytoplasmic 5' to 3' exonuclease Xrn1p is also a genome-wide transcription factor in yeast. *Frontiers in Genetics,5*(1), 1-10.

30. Sun, G., Liu, J., Li, G., Zhang, X., Chen, T., Zhang, H., . . . Pan, H. (2015). Quick and Accurate Detection and Quantification of Magnaporthe oryzae in Rice Using Real-Time Quantitative Polymerase Chain Reaction. *Plant Disease,99*(2), 219-224.

Appendix A

DATA VALUES

A.1 Raw Data Values for Growth Assays

Table A1 Values for Complete Media, Oatmeal, Minimal, and ROS Growth Rate Assays (in millimeters)

Mutant	Day 5	Day 6	Day 7	Day 8
Complete Media				
Δ*xrn1*-9	27.5	31.5	33.5	38
Δ*xrn1*-14	29	36.5	37.5	41
Δ*caf16*-11	29.5	37	41	44
Δ*caf16*-19	28	35	36	38
CAF16 EM	33	36	39	45
wt	27	33	35.5	39.5
Oatmeal Media				
Δ*xrn1*-9	23.5	28	29.5	38
Δ*xrn1*-14	24	28	29	36.5
Δ*caf16*-11	21	28.5	30.5	38
Δ*caf16*-19	21.5	25.5	29.5	36
CAF16 EM	23	29.5	31	39
wt	23	30	30	39.5
Minimal Media				
Δ*xrn1*-9	22.5	30	34	38.5
Δ*xrn1*-14	21.5	29	32	38
Δ*caf16*-11	24	34	37	42.5
Δ*caf16*-19	22	29	35	39
CAF16 EM	27.5	34	39	43.5
wt	24.5	31	35.5	39.5

Table A1 Values for Complete Media, Oatmeal, Minimal, and ROS Growth Rate Assays (in millimeters) (Continued)

ROS H2O2				
Δxrn1-9	26.5	32.5	34	39.5
Δxrn1-14	26	31.5	34.5	39
Δcaf16-11	23.5	31	36	41.5
Δcaf16-19	28	32	34	39
CAF16 EM	26	32	34	37.5
wt	26.5	33	34	37.5

Table A2 Values for Complete Media, Nitrogen Starved, and ROS Growth Rate Assays (in millimeters)

Mutant	Day 4	Day 5	Day 6	Day 7
Complete Media				
wt	16	23	29	35
CAF16-EM	17	25	31	36
Δ*xrn1*-9	17	23	29	37
Δ*xrn1*-14	18	23	29	32
Δ*caf16*-11	15	24	31	36
Δ*caf16*-19	17	23	29	36
Nitrogen Starved				
wt	10	12	16	21
CAF16-EM	9	11	15	15
Δ*xrn1*-9	8	11	15	19
Δ*xrn1*-14	11	14	18	22
Δ*caf16*-11	7	15	19	24
Δ*caf16*-19	8	16	20	20
ROS-10uM				
wt	11	21	27	35
CAF16-EM	16	21	26	32
Δ*xrn1*-9	15	21	28	34
Δ*xrn1*-14	16	22	29	35
Δ*caf16*-11	17	23	30	36
Δ*caf16*-19	18	24	31	36

Table A2 Values for Complete Media, Nitrogen Starved, and ROS Growth Rate Assays (in millimeters) (Continued)

ROS-100uM				
wt	11	16	20	24
CAF16-EM	11	14	18	21
Δ*xrn1*-9	12	17	21	27
Δ*xrn1*-14	15	20	26	30
Δ*caf16*-11	12	16	21	26
Δ*caf16*-19	12	18	23	30

A.2 Nanodrop Values for RNA Isolations of Mutants and Wild-type in Various Conditions

Table A3 Complete Media RNA Isolation Nanodrop Values for Growth Media Assay (Samples in Gray were used for cDNA synthesis)

1st Biological Replicate				**2nd Biological Replicate**			
Sample	ng/ul	260/280	260/230	**Sample**	**ng/ul**	**260/280**	**260/230**
wt1	5739	1.76	1.8	**wt1**	5101	1.94	1.71
wt2	4859	2	1.97	**wt2**	3091	2.11	1.28
***XRN1*-9-1**	1740	1.67	1.79	***XRN1*-9-1**	2377	2.15	1.41
***XRN1*-9-2**	6112	1.19	1.19	***XRN1*-9-2**	5040	1.97	1.57
***XRN1*-14-1**	6135	1.24	1.2	***XRN1*-14-1**	4611	2.01	2.1
***XRN1*-14-2**	5267	1.93	1.83	***XRN1*-14-2**	4135	2.04	1.91
***CAF16*-11-1**	4957	1.99	2.02	***CAF16*-11-1**	5816	1.69	1.49
***CAF16*-11-2**	6095	1.41	1.48	***CAF16*-11-2**	5760	1.74	1.78
***CAF16*-19-1**	6104	1.37	1.38	***CAF16*-19-1**	5856	1.4	1.32
***CAF16*-19-2**	6122	1.12	1.19	***CAF16*-19-2**	5997	1.63	1.68
***CAF16*-EM-1**	6104	1.29	1.22	***CAF16*-EM-1**	5686	1.78	1.19
***CAF16*-EM-2**	4886	1.99	2.07	***CAF16*-EM-2**	5706	1.77	1.83

Table A4 Minimal Media RNA Isolation Nanodrop Values for Growth Media Assay (Samples in Gray were used for cDNA synthesis)

1st Biological Replicate				**2nd Biological Replicate**			
Sample	ng/ul	260/280	260/230	**Sample**	**ng/ul**	**260/280**	**260/230**
wt1	900	2.01	0.59	**wt1**	2909	2.02	1.66
wt2	1923	2.01	1.2	**wt2**	1167	2.07	1.73
***XRN1*-9-1**	**436**	**2.02**	**0.62**	*XRN1*-9-1	**2200**	**2.01**	**0.56**
***XRN1*-9-2**	271	2.01	0.32	***XRN1*-9-2**	1333	2.04	0.46
***XRN1*-14-1**	1650	2.04	0.57	***XRN1*-14-1**	449	1.98	0.55
***XRN1*-14-2**	1415	2.06	1.19	***XRN1*-14-2**	1428	2.05	0.59
***CAF16*-11-1**	1021	2.07	0.98	***CAF16*-11-1**	1578	2.06	0.86
***CAF16*-11-2**	1614	2.01	0.38	***CAF16*-11-2**	2166	2.08	1.78
***CAF16*-19-1**	690	2.05	0.34	***CAF16*-19-1**	2924	2.08	2.04
***CAF16*-19-2**	1292	2.03	1.27	***CAF16*-19-2**	456	1.97	0.53
***CAF16*-EM-1**	626	2.04	0.31	***CAF16*-EM-1**	1887	2.07	1.71
***CAF16*-EM-2**	1147	2.05	0.53	***CAF16*-EM-2**	456	1.97	0.49

Table A5 ROS (10μM) Media RNA Isolation Nanodrop Values for Growth Media Assay (Samples in Gray were used for cDNA synthesis)

1st Biological Replicate				**2nd Biological Replicate**			
Sample	**ng/ul**	**260/280**	**260/230**	**Sample**	**ng/ul**	**260/280**	**260/230**
wt1	3211	1.83	1.22	**wt1**	1676	2.17	1.16
wt2	5805	1.59	1.42	**wt2**	5967	1.56	1.52
***XRN1*-9-1**	4926	1.99	1.8	***XRN1*-9-1**	5030	1.96	1.41
***XRN1*-9-2**	4914	1.95	1.34	***XRN1*-9-2**	5294	1.88	1.06
***XRN1*-14-1**	1453	2.16	0.93	***XRN1*-14-1**	6168	1.17	1.14
***XRN1*-14-2**	4915	1.97	1.84	***XRN1*-14-2**	5636	1.62	1.06
***CAF16*-11-1**	5905	1.66	1.65	***CAF16*-11-1**	129	1.99	0.17
***CAF16*-11-2**	2548	1.97	1.57	***CAF16*-11-2**	5381	1.9	1.96
***CAF16*-19-1**	4624	2.03	2.09	***CAF16*-19-1**	2486	2.08	2.02
***CAF16*-19-2**	911	2.13	1.59	***CAF16*-19-2**	5008	1.95	1.25
***CAF16*-EM-1**	199	2	0.3	***CAF16*-EM-1**	4228	2.01	1.32
***CAF16*-EM-2**	1479	2.09	1.72	***CAF16*-EM-2**	6000	1.57	1.31

Table A6 Complete Media Nanodrop Values to Test Primers for *POR1*/*DCS1* (Samples in Gray were used for cDNA synthesis) (1st set of Technical Replicates)

Sample	**ng/ul**	**260/280**	**260/230**
wt1	3630	2.06	1.54
wt2	3620	2.05	1.94
***XRN1*-9-1**	1589	2.14	2.41
***XRN1*-9-2**	3181	2.1	2.3
***XRN1*-14-1**	5612	1.77	1.84
***XRN1*-14-2**	6000	1.11	1.24
***CAF16*-11-1**	4895	1.97	1.68
***CAF16*-11-2**	659	2.08	2.08
***CAF16*-19-1**	5033	1.98	1.97
***CAF16*-19-2**	5896	1.71	1.63
***CAF16*-EM-1**	6070	1.2	1.25
***CAF16*-EM-2**	5939	1.29	1.35

Table A7 Complete Media RNA Isolations for *DCS1*/*POR1* Analysis (Samples in Gray were used for cDNA synthesis) (1st Set of Technical Replicates)

Sample	ng/ul	260/280	260/230
wt1	853	1.74	0.59
wt2	341	1.79	0.56
wt3	5027	1.84	1.34
wt4	4866	1.87	1.28
***XRN1*-9-1**	5263	1.9	1.71
***XRN1*-9-2**	2076	2.04	1.8
***XRN1*-9-3**	4068	1.99	1.79
***XRN1*-9-4**	5929	1.58	1.49
***XRN1*-14-1**	3610	2	1.65
***XRN1*-14-2**	854	2	1.57
***XRN1*-14-3**	2111	2.04	1.81
***XRN1*-14-4**	1973	2	1.42
***CAF16*-11-1**	1291	1.89	0.93
***CAF16*-11-2**	1261	1.93	1.04
***CAF16*-11-3**	1598	2	1.34
***CAF16*-11-4**	4003	1.98	1.53
***CAF16*-19-1**	2508	2.01	1.4
***CAF16*-19-2**	4500	1.96	1.61
***CAF16*-19-3**	2410	2.01	1.51
***CAF16*-19-4**	4279	1.97	1.6
***CAF16*-EM-1**	2574	1.93	0.95
***CAF16*-EM-2**	3219	1.93	1.01
***CAF16*-EM-3**	1324	1.75	0.58
***CAF16*-EM-4**	6057	1.61	1.46

Table A8 Complete Media RNA Isolations for *DCS1*/*POR1* Analysis (Samples in Gray were used for cDNA synthesis) (1st Set of Technical Replicates)

Sample	**ng/ul**	**260/280**	**260/230**
XRN1-9-1	145.6	1.96	0.73
XRN1-9-2	--	--	--
XRN1-14-1	96.4	1.78	0.82
XRN1-14-2	79.4	1.78	1
CAF16-11-1	321.1	1.98	1.88
CAF16-11-2	137.4	1.76	1.12
CAF16-19-1	3231.2	2.08	2.21
CAF16-19-2			
CEM 1	144.6	1.88	1.21
CEM 2	5863	1.66	1.7
WT-1	1040	2.05	2.09
WT-2	5303	1.89	2.02

A.3 qPCR Analysis of *DCS1* in mutants (p> 0.05)

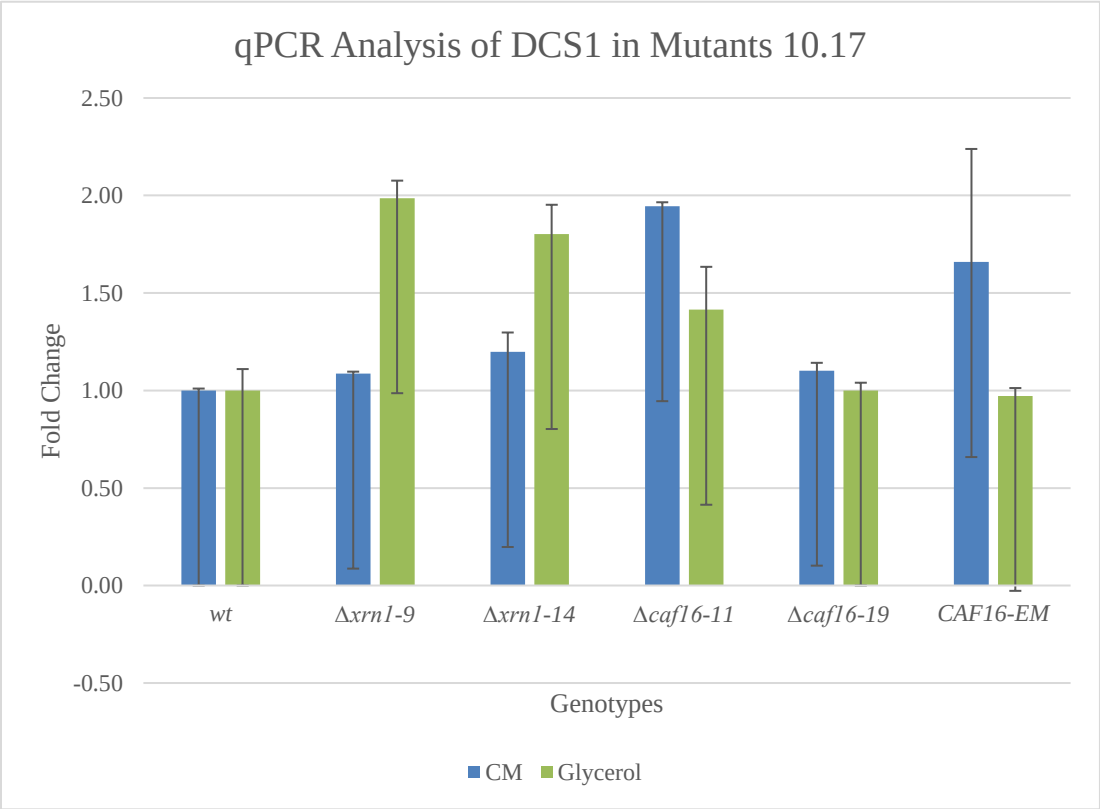

Figure A1 - qPCR Analysis of *DCS1* in mutants using Primers EV72 and EV73. Standard error bars are based on two technical replicates. Based on a student t-test, this data is not statistically significant (p >0.05).

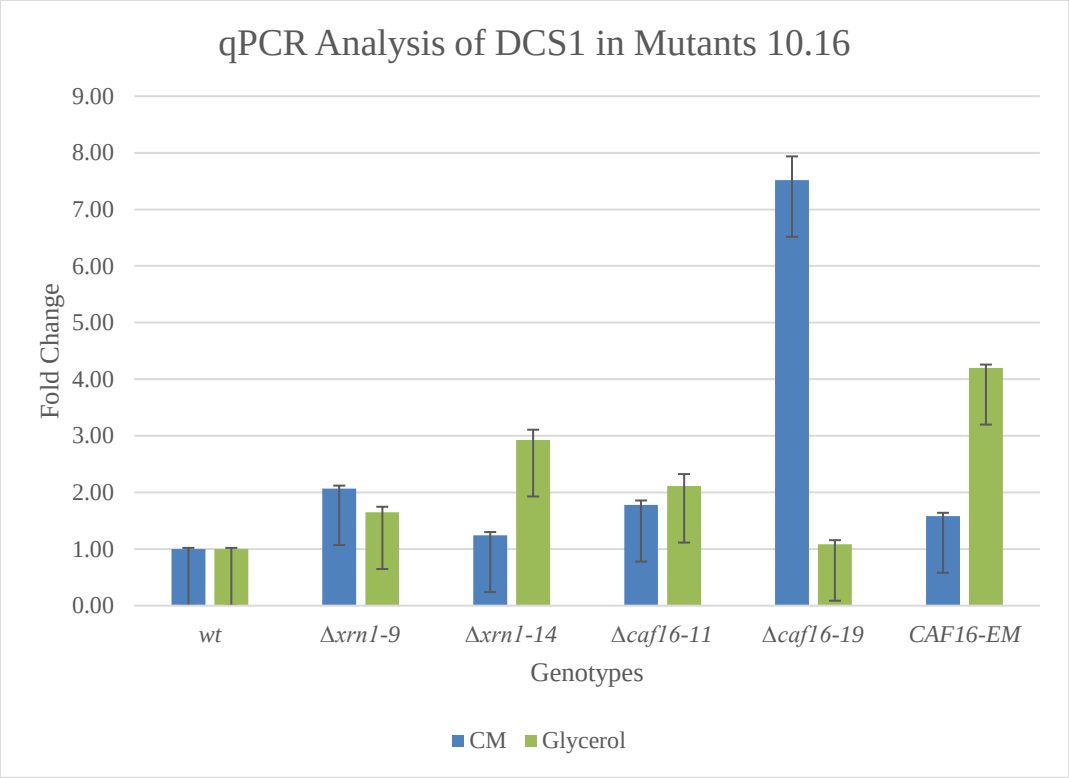

Figure A2 qPCR Analysis of *DCS1* in mutants using Primers EV74 and EV75. Standard error bars are based on two technical replicates. Based on a student t-test, this data is not statistically significant ($p > 0.05$).

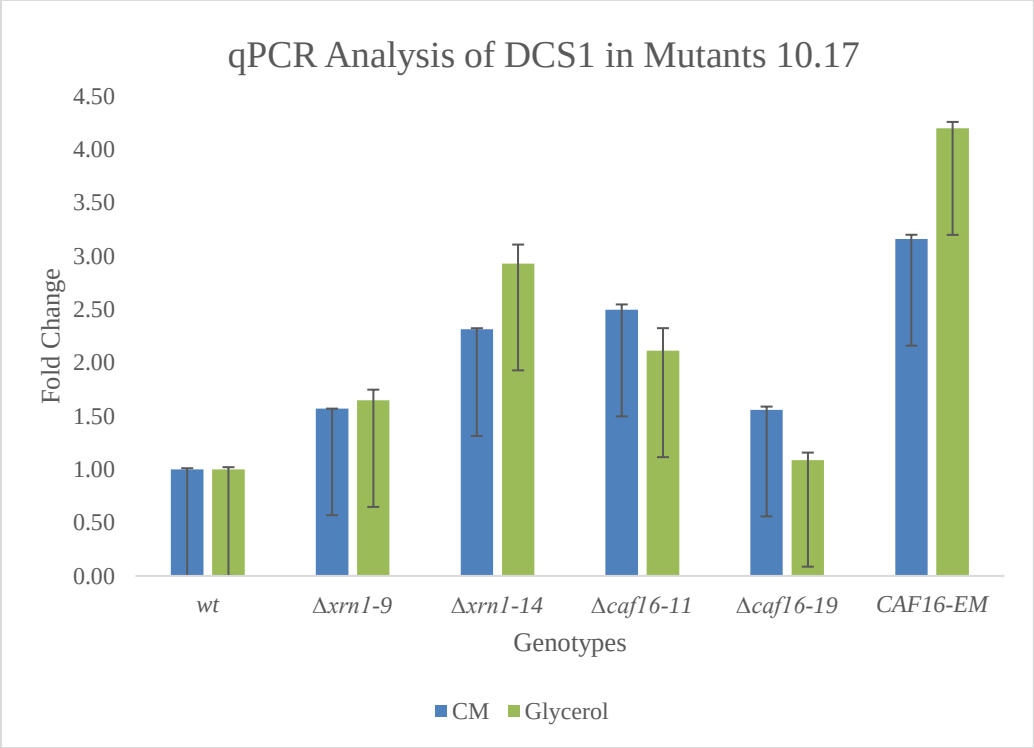

Figure A3 Second Biological Replicate. qPCR Analysis of *DCS1* in mutants using Primers EV74 and EV75. Standard error bars are based on two technical replicates. Based on a student t-test, this data is not statistically significant ($p > 0.05$).

A.4 qPCR Analysis of *POR1* in mutants (p>0.05)

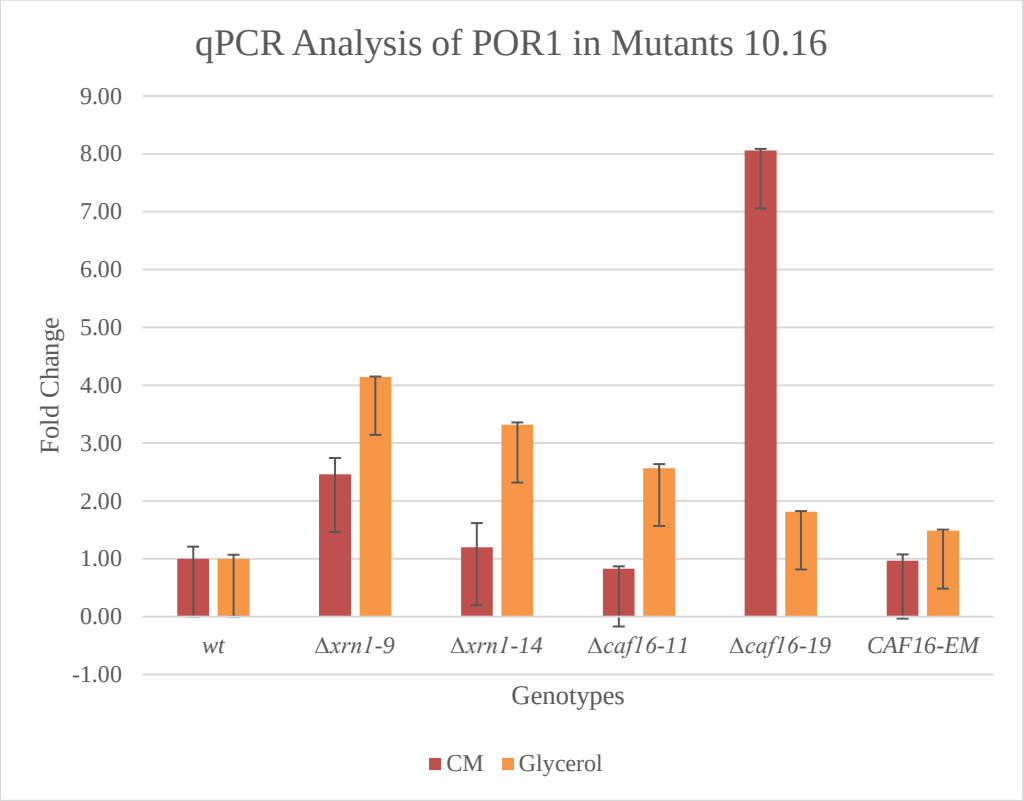

Figure A4 qPCR Analysis of *POR1* in mutants using Primers EV80 and EV81. Standard error bars are based on two technical replicates. Based on a student t-test, this data is not statistically significant (p >0.05).

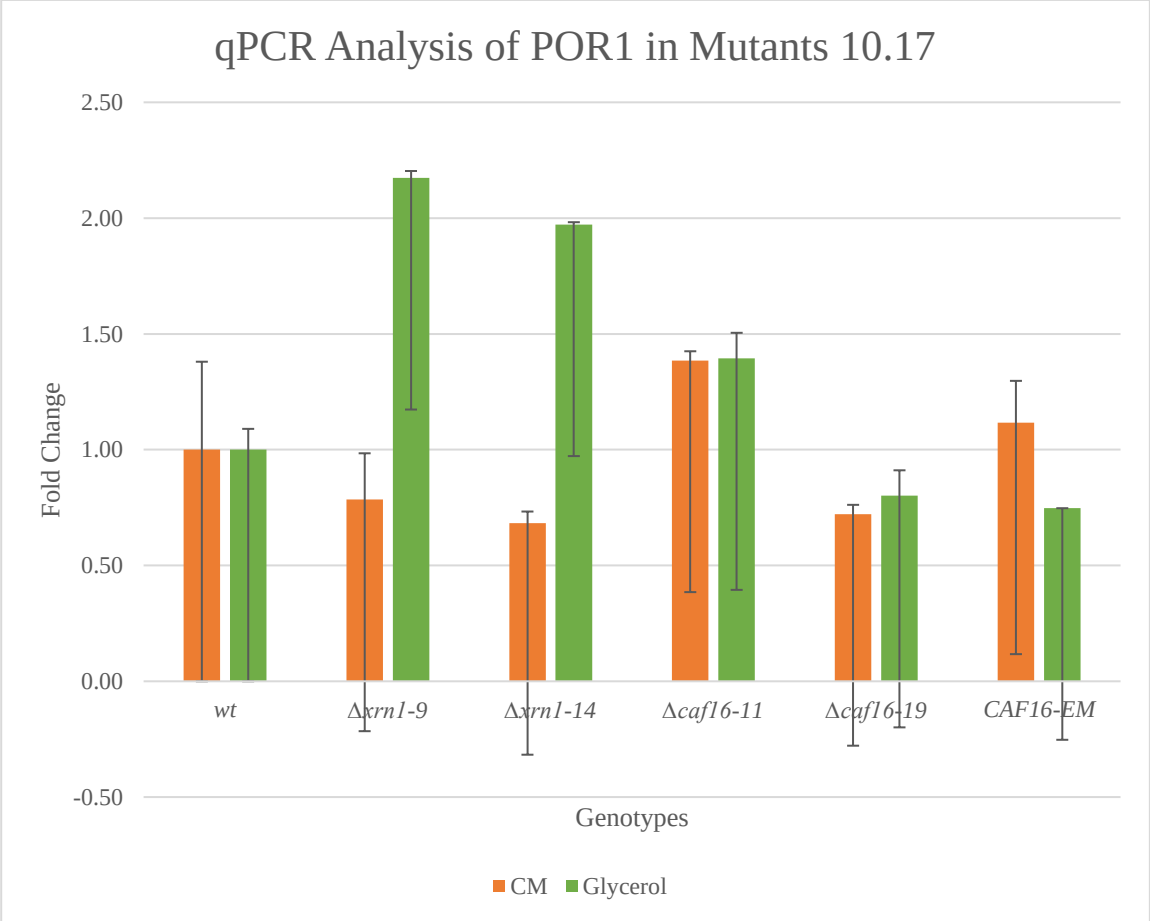

Figure A5 qPCR Analysis of *POR1* in mutants using Primers EV82 and EV83. Standard error bars are based on two technical replicates. Based on a student t-test, this data is not statistically significant ($p > 0.05$).

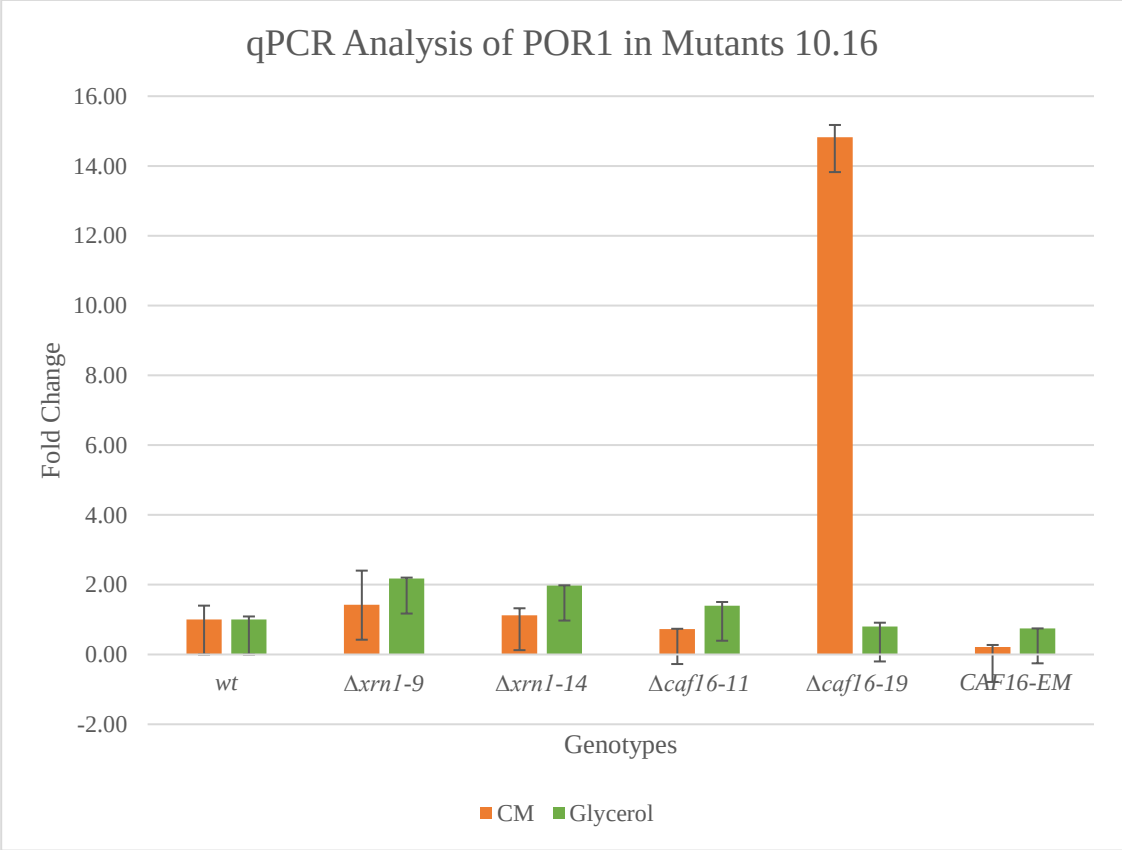

Figure A6 qPCR Second Biological Replicate Analysis of *POR1* in mutants using Primers EV82 and EV83. Standard error bars are based on two technical replicates. Based on a student t-test, this data is not statistically significant ($p > 0.05$).